Numerical Methods in Civil Engineering

A New Efficient Form of The Modified Energy Method (MEM) in Structural Dynamics

Mohammad. Jalili Sadr Abad[*], **Mussa. Mahmoudi**[**]

ARTICLE INFO

Article history:
Received:
June 2018.
Revised:
August 2018.
Accepted:
September 2018.

Keywords:
Modified Energy Method;
Time integration method;
Nonlinear Structural Dynamics;
Stability

Abstract:

The selection of a suitable numerical method to evaluate the dynamic behavior of structures, especially in nonlinear cases, is an important task in practice. Accordingly, the purpose of this study is to demonstrate the numerical features of a new single-step type of the Modified Energy Method (MEM) to compute the dynamic response of structural systems. A comprehensive formulation of this energy-based time integration scheme to incorporate the general nonlinear behavior in MDOF systems is presented for the first time ever in this paper. After discussing the stability and accuracy of the proposed time-stepping integration procedure, five applicable numerical examples in structural dynamics and earthquake engineering practices involving the various hysteretic behaviors and the effects of consistent mass and non-classical damping matrices are examined by the presented technique. In each case, the relevant comparisons are given in accordance to other available methods (e.g., Newmark and Runge-Kutta). Overall, the results indicate that the MEM yields a better accuracy than the 2nd Runge-Kutta approach. Furthermore, the distinguishing feature of the proposed method is to provide information about choosing the optimal size of the time intervals, especially in the nonlinear analyzes, which is not achievable in other applicable approaches.

1. Introduction

Although nonlinear dynamics analysis disseminate a more realistic behavior of the structure to the analyst; but it is inherently complex since there is no closed-form solution in most cases. One of the main drawbacks in analyzing theses type of problems is the lack of application of the superposition principle that is widely used in computing the response of linear systems. For example, many of the concepts in the dynamics of linear structures such as the usage of Duhamel integrals, integral transform maps (e.g., Laplace, Fourier), as well as the popular modal analysis method cannot be applied when we are dealing with the dynamics related problems within nonlinear terms. Consequently, for the practical engineering works, numerical methods are used to approximate the exact response of a nonlinear initial value problem (IVP). Undoubtedly, the most important factor in utilizing a numerical method is its efficiency.

**Corresponding Author: Ph.D. graduated of Structural Engineering, Department of Civil Engineering, Shahid Rajaee Teacher Training University, Tehran, Iran. E-mail: m.jalili@sru.ac.ir*

*** Associate Professor, Department of Civil Engineering, Shahid Rajaee Teacher Training University, Tehran, Iran.*

The efficacy of a numerical method in the structural dynamics analysis can be studied by some factors such as comprehensiveness, stability, accuracy, computational cost, simple computer implementations, needlessness in defining the additional parameters, self-starting, and so on. Nevertheless, it has to be noted that each one of the current methods has its advantages and disadvantages.

Direct time integration methods (DTIMs) are the most commonly used in practice to determine the dynamic response of structures. The constant acceleration (trapezoidal rule), linear acceleration, and central difference methods are three traditional techniques in this context (Bathe 2014[3]). Historically, Houbolt (1950[14]) presented a three-step time integration scheme to analyze the forced vibration in aerospace structures. The most significant disadvantage of this method is its non-self-starting nature, and it has also been proven that the method is less accurate than other integration techniques (Wen *et al.* 2017[35]). Newmark (1959[27]) also proposed a numerical time integration method by

introducing the two parameters γ and β in order to adjust the stability and accuracy of the solution.

However, in the case of the linear acceleration, the method was conditionally stable; hence, Wilson *et al*. (1973[36]), with defining an additional integral parameter, denoted as θ, introduced another numerical technique to make the linear acceleration method of Newmark unconditionally stable. Collocation methods that are basically the combination of the Wilson and Newmark methods, with three additional parameters (γ, β, θ), are of another category that were invented later (Kolay & Ricles, 2014[21]). Subsequently, Hilber *et al*. (1977[13]) proposed the HHT-α method in order to have a controllable numerical damping method, where the kinematic relations are the same, as the Newark method. Chung and Hulbert (1993[8]), by generalizing the HHT method, were seeking an optimal numerical damping control to eliminate the unwanted frequencies in the response of a dynamic system.

In the recent years, many DTIMs have also been developed based on the concepts of time finite element approach. For example, Shojaee *et al*. (2015[32]) developed an unconditionally stable implicit form, by modifying a conditionally stable explicit method based on the quartic B-spline polynomials which were used in Ref. (Rostami *et al.* 2012[31]). Zhang *et al*. (2015[37]) work on a composite time integration method based on the three-point Forward Euler formula with a generalized central differential formulation for nonlinear analysis of structures. In another study carried out by Cilsalar and Aydin (2016[9]) by employing the weighted residuals approach in violation of the assumption of linear acceleration in their time-integration method, investigated the effect of parabolic and cubic variations of acceleration on the analysis of nonlinear dynamic problems. Furthermore, Kim and Choi (2016[19];2018[20]) introduced a new implicit technique based on the weighted residual method (WRM) by introducing one free parameter that controls algorithmic dissipation. They reported that their algorithm is more accurate compared to the Bathe method. In general, in these type of approaches, and for the stability conditions there is no general condition to guarantee the stability of the method of integration in nonlinear problems (Park 1975[28]; Zienkiewicz *et al.* 2014[38]; Belytschko *et al.* 2014[6]).

Generally, all DTIMs are conducting based on the solution of the second-order equation of motion. However, the energy balance equations can be considered in the evaluation of the dynamic response of structural systems. For example, Kuhl and Crisfield (1999[23]) have studied the energy conservation algorithms in nonlinear dynamics of structures; while, Bathe (2007[1]) reported the loss of energy conservation in some nonlinear dynamic analysis using the Newark method. Farhat *et al*. (2015[11]) worked on the Structure-preserving, stability, and accuracy properties of the energy-conserving sampling and weighting method for the hyper reduction of nonlinear finite element dynamic models. Besides, the energy balance method (EBM) that is used to determine the approximate response of nonlinear oscillators can be mentioned in this regard (Bayat *et al*. 2016[5]). He (2002[12]) thoroughly investigated the usage of the Hamilton principle to calculate the frequency of nonlinear oscillators through some numerical problems. In that regard, Khan and Mirzabeigy (2014[18]) introduced the improved energy balance method (IEBM) in order to increase the accuracy of the EBM in the analysis of conservative nonlinear oscillators. Indeed, they used an extended trial function based on Galerkin's method in their work. In another similar study, for achieving a higher-order approximation of the solution of such problems Razzak and Rahman (2015[29]), by defining a higher-order trial function studied some strongly nonlinear oscillator systems. Furthermore, Navarro and Cveticanin (2016[26]) also tried to calculate the amplitude-frequency relationship by means of the Hamiltonian principle regarding oscillators with the sum of non-integer order nonlinearities. The solution of the nonlinear differential equation was based on the assumption of a trigonometric function with an unknown frequency, and the frequency equation is obtained by inserting the Hamiltonian's derivative equal to zero. The obtained results were also verified by analytical solutions and the development of an error estimation method on the basis of the relationship between the average residual function and the total energy of the system.

Overall, by reviewing the preceding literature, it can be seen that for the direct time integration methods, there is a need to select and adjust the additional integration parameters (β,γ,θ,α). The recommended values for selecting these parameters are based on the very simple assumptions, such as the case of linear and free vibration. The energy balance methods also create very complex mathematical expressions with many limitations especially their limited application for SDOF systems. In other words, these approaches can only be useful in finding the approximated natural frequency of some nonlinear oscillators; so, the time-history response of a general nonlinear structure cannot be obtained via these methods. Moreover, none of the DTIMs and EBMs can provide the analyst with the appropriate information about the choice of the appropriate size of time steps to analyze a nonlinear problem. Accordingly, this paper aims to present a comprehensive form of an energy-based time integration method, denoted as Modified Energy Method (MEM), to overcome the aforementioned drawbacks.

This method with the quadratic form is able to consider the effect of loading, the system's damping, as well as the duration of the analysis on the selection of the optimum Δt. It is to be noted that the basic idea of the presented method is initially stated in (Jalili Sadr Abad *et al*. 2017[16]) as a composite and iterative formulation which was based on the simultaneous usage of force and equilibrium equations. This method was named as the Modified Energy Method (MEM) applied to the SDOF systems with different nonlinearities. Subsequently, this approach is generalized to the linear analysis of the shear-frames as one of the practical MDOF structures, where a mathematical technique (EDV) was for the first time proposed in (Jalili Sadr Abad *et al*. 2018[17]) to numerically solve the set of quadratic and coupled discretized equations.

In the current work, in order to demonstrate the comprehensiveness of the method for analyzing various problems in the dynamics of structures, a new single-step form for MEM is introduced. Employing different first-order integration techniques (forward- and backward-Euler, as well as trapezoidal rule), stability and accuracy analysis of the method, considering the non-diagonal/consistent mass matrix and non-proportional damping effects, as well as the analysis of nonlinear MDOF systems, together with discussion on choosing the optimum size of time step in a nonlinear analysis, are some of the novelties for the present study compared to the previous works.

2. Different force-based methods of analysis in structural dynamics

The following general form can express the second-order differential equation of motion of an oscillator.

$$m\ddot{u} + c\dot{u} + fs(u,\dot{u}) = F \tag{1}$$

where, m, c, f_S, and F are respectively the mass, damping, nonlinear restoring force, and external force of the system. u also denotes the displacement of the vibrating system, and the dot represents the time derivative.

Generally, there are two different approaches in practice and in the numerical solution of this type of nonlinear equation. For the first category, an incremental form of the equation of motion is used, and then a direct integration method (e.g., Newmark) is used along with an iterative method like Newton-Raphson. Alternatively, by rewriting Eq. (1) in a system of first-order equations (state-space form), the time-history response of the system can be determined using one of the commonly used first-order numerical integrating techniques such as Runge-Kutta method. In the following section, each of these two methods is illustrated in more details.

2.1. Direct time integration method (incremental force equilibrium equation)

If we subtract the force equilibrium of the system at time t from the same equation at time $t+\Delta t$, we will get the following incremental force equilibrium. Note that m and c are assumed to be constants throughout this study.

$$m\Delta\ddot{u} + c\Delta\dot{u} + \Delta fs = \Delta F \tag{2}$$

In the step-by-step time integrating methods, by defining an instantaneous stiffness, k_t, the stiffness of the system during the analysis will be updated. Hence, the variation of restoring force between two consecutive time steps is given by

$$\Delta fs = k_t . \Delta u \tag{3}$$

In these cases, to obtain the response history, the time domain is divided into small intervals, Δt. Then, in each of these time intervals, by assuming constant dynamic properties of the structure, a suitable kinematic assumption must be made (such as linear or constant acceleration) to compute the system's response. In the following, we will focus on the family of Newark methods that are widely used in practice. In this situation, displacement and velocity at time $t=t_{j+1}$, respectively, are expressed by Eqns. (4) and (5).

$$u_{j+1} = u_j + \Delta t\dot{u}_j + \frac{\Delta t^2}{2}[(1-2\beta)\ddot{u}_j + 2\beta\ddot{u}_{j+1}] \tag{4}$$

$$\dot{u}_{j+1} = \dot{u}_j + \Delta t[(1-\gamma)\ddot{u}_j + \gamma\ddot{u}_{j+1}] \tag{5}$$

in which β and γ are the acceleration coefficients in the calculation of velocity and displacement. Table 1 represents the different forms of Newmark's integration methods for various combinations of β and γ, where $T_{\min}$ denotes the fundamental period of the vibrational system. Here, it should be mentioned that the stability condition given in Table 1 is only valid for linear systems and there is no proven stability condition for nonlinear analyses for the time integration methods. As already stated, one of the problems that we are faced in practice with methods such as Newmark, especially in nonlinear analyzes, is the choice of appropriate values or the calibration of these integral constants.

Table 1. Newmark family of time integration methods (Kolay & Ricles 2016[22])(Soroushian, 2017[33])

Time integration method	β	Formula	Stability condition	Type of formula
Central difference	0	$u_{i+1} = u_i + h\dot{u}_i + \frac{h^2}{2}\ddot{u}_i$	$h \le \frac{T_{min}}{\pi}$	Explicit
Fox-Goodwin	1/12	$u_{i+1} = u_i + h\dot{u}_i + \frac{h^2}{2}[\frac{5}{6}\ddot{u}_i + \frac{1}{6}\ddot{u}_{i+1}]$	$h \le \frac{\sqrt{6}}{2\pi}T_{min}$	implicit
Linear acc.	1/6	$u_{i+1} = u_i + h\dot{u}_i + \frac{h^2}{2}[\frac{2}{3}\ddot{u}_i + \frac{1}{3}\ddot{u}_{i+1}]$	$h \le \frac{\sqrt{12}}{2\pi}T_{min}$	implicit
Average acc.	1/4	$u_{i+1} = u_i + h\dot{u}_i + \frac{h^2}{2}[\frac{1}{2}\ddot{u}_i + \frac{1}{2}\ddot{u}_{i+1}]$	unconditional	implicit
Backward acc.	1/2	$u_{i+1} = u_i + h\dot{u}_i + \frac{h^2}{2}\ddot{u}_{i+1}$	unconditional	implicit

2.2. State-Space Approach (First-Order System of Differential Equations)

By introducing a state-vector $[x_1, x_2]^T$ where x_1 and x_2 are the displacement and velocity of the oscillator, the second-order differential equation of motion, Eq.(1), can be reduced into a first-order system as follows.

$$\begin{Bmatrix} \dot{x}_1 \\ \dot{x}_2 \end{Bmatrix} = \begin{Bmatrix} x_2 \\ m^{-1}[F - cx_2 - fs(x_1, x_2)] \end{Bmatrix} \quad (6)$$

In general, in the case of *n*-DOF systems, 2*n* first-order differential equations will be obtained by transforming from *n* second-order differential equations of motion. These equations can be expressed in a vector form as below.

$$\dot{\mathbf{x}} = \mathbf{f}(\mathbf{x}, t) \quad (7)$$

Most of the times, in order to solve these forms of first-order vector equations, after the discretization in time, the state of the system at the current time $\mathbf{x}_{j+1}$ is obtained from the system's state at time t_j, plus some increment, $d\mathbf{x}$, i.e.

$$\mathbf{x}_{j+1} = \mathbf{x}_j + d\mathbf{x} \quad (8)$$

As a favorite technique, for the second-order Range-Kutta (RK2) method, one can write

$$d\mathbf{x} = \frac{\Delta t}{2}[\mathbf{f}(t_j, \mathbf{x}_j) + \mathbf{f}(t_j + \Delta t, \mathbf{x}_j + \Delta t.\mathbf{f}(t_j, \mathbf{x}_j))] + O(\Delta t^3) \quad (9)$$

Additionally, for the fourth-order Range-Kutta method (RK4), we have

$$d\mathbf{x} = \frac{1}{6}[\mathbf{k}_1 + 2\mathbf{k}_2 + 2\mathbf{k}_3 + \mathbf{k}_4] + O(\Delta t^5)$$

$$\mathbf{k}_1 = \Delta t\,\mathbf{f}(t_i, \mathbf{x}_i);$$

$$\mathbf{k}_2 = \Delta t\,\mathbf{f}(t_i + \frac{\Delta t}{2}, \mathbf{x}_i + \frac{\mathbf{k}_1}{2}); \quad (10)$$

$$\mathbf{k}_3 = \Delta t\,\mathbf{f}(t_i + \frac{\Delta t}{2}, \mathbf{x}_i + \frac{\mathbf{k}_2}{2});$$

$$\mathbf{k}_4 = \Delta t\,\mathbf{f}(t_i + \Delta t, \mathbf{x}_i + \mathbf{k}_3)$$

It should be noted that RK2 belongs to single-step time integration methods; but, RK4 is a multi-step method that uses a sub-step to increase the accuracy of the solution. Hence, the RK4 method is more computationally expensive than RK2. Generally, here it is worth mentioning that the main weak point of these kind of methods (viz. state-space approaches) is the incorporation with non-diagonal/consistent mass matrices in vibrational systems. This point will be elaborated and discussed later.

3. Research methodology

In the following section, the concepts of the new single-step form of Modified Energy Method (MEM) are illustrated in details. This formulation is first derived for SDOF systems; then, it is generalized to involve the general nonlinear behavior in an MDOF vibrating system. Finally, the stability and accuracy of the proposed numerical technique are discussed at the end of this section.

3.1. The incremental form of the energy balance equation for SDOF systems

Due to the changes in the dynamic properties of the system (e.g., stiffness) during nonlinear analysis, the usage of an incremental form of energy balance equations is always preferred in practice.

$$\Delta E_K + \Delta E_D + \Delta E_P = \Delta E_F \quad (11)$$

in which ΔE_K, ΔE_D, ΔE_P, and ΔE_F denote the variation of kinetic, dissipated/damped, potential, and loading energies in two consecutive times of t_j and t_{j+1} respectively.

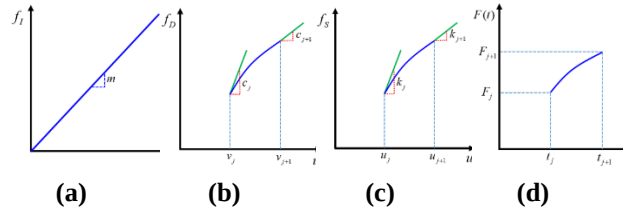

(a) **(b)** **(c)** **(d)**

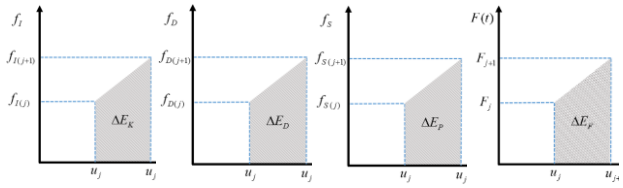

Fig. 1: Definition of various types of dynamical forces and corresponding energies: (a) Inertia force and kinetic energy; (b) Damping force and dissipated energy; (c) Spring force and potential energy; (d) External force and loading energy.

According to Figure 1(a), the variation of kinetic energy in the system can be written in the following form.

$$\Delta E_K = \int_{u_j}^{u_{j+1}} f_I du \xrightarrow{f_I=m\ddot{u}} \int_{u_j}^{u_{j+1}} m\ddot{u}du \xrightarrow{\ddot{u}du=vdv} = \frac{1}{2}m\left[v_{j+1}^2 - v_j^2\right] \quad (12)$$

where v_{j+1} and v_j respectively are the velocity of the object at times t_{j+1} and t_j.

By introducing the tangential damping coefficients (c_j,c_{j+1}) at the beginning and end of the time interval, as shown in Figure 1(b), the dissipated energy changes can be written using the trapezoidal rule as follows.

$$\Delta E_D = \int_{u_j}^{u_{j+1}} f_D du = \int_0^t f_D(v).v(t)\,dt = \frac{\Delta t}{2}[c_{j+1}v_{j+1}^2 + c_j v_j^2] \quad (13)$$

Similarly, the variations of potential energy for a nonlinear spring can also be written by defining instantaneous or tangential stiffness (k_j,k_{j+1}) at times t_{j+1} and t_j as displayed in Figure 1(c). We get,

$$\Delta E_P = \int_{u_j}^{u_{j+1}} f_S du = \frac{1}{2}k_{j+1}u_{j+1}^2 - \frac{1}{2}k_j u_j^2 \quad (14)$$

Finally, regarding Figure 1(d), the variation of external work related to loading is given by Eq.(15) with the use of the trapezoidal rule.

$$\Delta E_F = \int_{u_j}^{u_{j+1}} F(t)du = \int_{t_j}^{t_{j+1}} F(t)v(t)dt = \frac{\Delta t}{2}\left[F_{j+1}v_{j+1} + F_{j+1}v_j\right] \quad (15)$$

Consequently, by plugging the relations (12)-(15) in Eq.(11), the discretized form of the energy balance equation for a single-degree-of-freedom system is obtained as follows.

$$m\left[v_{j+1}^2 - v_j^2\right] + \Delta t[c_{j+1}v_{j+1}^2 + c_j v_j^2] + k_{j+1}u_{j+1}^2 - k_j u_j^2 = \Delta t\left[F_{j+1}v_{j+1} + F_{j+1}v_j\right] \quad (16)$$

Given the state of the system at time t=t_j, the above quadratic equation has two unknowns parameters (v_{j+1},u_{j+1}); therefore, it is necessary to relate the displacement at the current time with a kinematic relation to the velocity at the same time. Accordingly, Euler's formula might be utilized as follows.

$$u_{j+1} = u_j + \Delta t[(1-r)v_j + (r)\,v_{j+1}] \quad (17)$$

where r is a coefficient as of the range [0,1], which is conceptually the participation of the two current and former velocities (at the beginning and the end of the time-step) for computing the displacement at the current time. According to Table 2, different well-known forms of first-order time integration schemes can be achieved for various values of r. It should be noted that in the next sections, by performing different analyzes, the appropriate value to have a proper numerical response will be examined.

Table 2. Different forms of first-order approximation for three values of r

Forward Euler (r=0)	Crank-Nicolson (r=0.5)	Backward Euler (r=1)
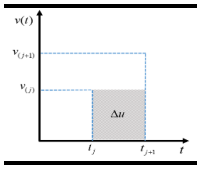	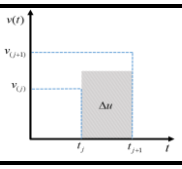	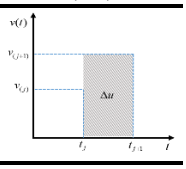
$u_{j+1} = u_j + \Delta t.v_j$	$u_{j+1} = u_j + 0.5\Delta t(v_{j+1} + v_j)$	$u_{j+1} = u_j + \Delta t.v_{j+1}$

Therefore, in order to find the system's response at time t_{j+1}, (u_{j+1},v_{j+1}), we must simultaneously solve two equations with two unknowns derived from the combination of equations (16) and (17), that is

$$m\left[v_{j+1}^2 - v_j^2\right] + \Delta t[c_{j+1}v_{j+1}^2 + c_j v_j^2] + k_{j+1}u_{j+1}^2 - k_j u_j^2 = \Delta t\left[F_{j+1}v_{j+1} + F_{j+1}v_j\right] \quad (18.a)$$

$$u_{j+1} = u_j + \Delta t[(1-r)v_j + (r)\,v_{j+1}] \quad (18.b)$$

In order to have an explicit form of the equation, substituting the second expression into the first one in Eq.(18), with some mathematical simplifications, the characteristic quadratic equation for v_{j+1} can be obtained as below.

$$Av_{j+1}^2 + Bv_{j+1} + C = 0$$

$$A = m + c_{j+1}\Delta t + k_{j+1}\Delta t^2 r^2$$

$$B = 2k_{j+1}\Delta t\, r\, u_j + 2k_{j+1}\Delta t^2 r(1-r)v_j - \Delta t F_{j+1} \quad (19)$$

$$C = (k_{j+1} - k_j)u_j^2 + v_j[-m\,v_j + c_j\,\Delta t\,v_j + k_{j+1}\Delta t^2(1-r)^2 v_j + 2k_{j+1}\Delta t(1-r)u_j - \Delta t F_j]$$

It can be seen from these relationships that the coefficient A is only a function of dynamical properties of the system (m,c,k) and integrating variables (r,Δt); but, the coefficients B and C vary with the state of system in the

previous step (u_j,v_j) and loading function (F), as well. Furthermore, an interesting point with regard to Eq.(19) is that the Delta (B^2-4AC) in this equation must always be a non-negative value to avoid creating non-imaginary velocities in the analysis procedure; hence, it can provide for the analyst a stability condition. For this purpose, the value of Δt must be lower than a specific limit, which is the function of the dynamic properties, the discrete variables, and also the external load. Nevertheless, this issue will be discussed later in future sections.

3.2. Detection of the Actual System's Velocity

Now assuming $B^2 > 4AC$, solving quadratic Eq.(19) gives two roots as follows.

$$Av_{j+1}^{2} + Bv_{j+1} + C = 0 \rightarrow v_{j+1}^{(1)} = \frac{-B+\sqrt{\Delta}}{2A}, v_{j+1}^{(2)} = \frac{-B-\sqrt{\Delta}}{2A} \quad (20)$$

However, the physical system only has a unique velocity at any given time. As a result, the real and spurious velocity of the system should be identified at any time. For this purpose, one may use the better forces equilibrium by estimation of acceleration by Eq.(21), as below

$$a_{j+1}^{(1)} = \frac{v_{j+1}^{(1)} - v_j}{\Delta t} \quad , \quad a_{j+1}^{(2)} = \frac{v_{j+1}^{(2)} - v_j}{\Delta t} \quad (21)$$

In Eq.(21), two corresponding accelerations ($a_{j+1}^{(1)}$, $a_{j+1}^{(2)}$) are assessed from two calculated velocities at time t_{j+1} ($v_{j+1}^{(1)}$, $v_{j+1}^{(2)}$) and the velocity of the previous time step (v_j).

Then, by checking Eq.(22), the velocity with a better force equilibrium is selected as the real velocity of the system (v_{real}). Mathematically,

$$v_{real} = \begin{cases} v_{j+1}^{(1)} & \text{if} \quad f_1 < f_2 \\ v_{j+1}^{(2)} & \text{otherwise} \end{cases} ; \quad (22)$$

$$f_1 = \left| m a_{j+1}^{(1)} + \overline{c}\, v_{j+1}^{(1)} + \overline{k}\, x_{j+1}^{(1)} - F_{j+1} \right|$$

$$f_2 = \left| m a_{j+1}^{(2)} + \overline{c}\, v_{j+1}^{(2)} + \overline{k}\, x_{j+1}^{(2)} - F_{j+1} \right|$$

Given that the value of Δt is usually very small in practical analyzes, a key idea to be utilized here is that by taking $\Delta t \rightarrow 0$ in Eq.(22) and ignoring other terms against the first term, we can achieve an interesting result that can possess a physical interpretation. In this situation, Eq.(22) takes the form

$$v_{real} = \begin{cases} v_{j+1}^{(1)} & \text{if} \quad e_1 < e_2 \\ v_{j+1}^{(2)} & \text{otherwise} \end{cases} ; \quad (23)$$

$$e_1 = \left| v_{j+1}^{(1)} - v_j \right| \quad , \quad e_2 = \left| v_{j+1}^{(2)} - v_j \right|$$

In this equation, $\left| v_{j+1}^{(1)} - v_j \right|$ and $\left| v_{j+1}^{(1)} - v_j \right|$ could express the distance between the calculated velocities at the current time (t_{j+1}) and the velocity at the preceding time step (t_j). This technique, which is first introduced in (Jalili Sadr Abad *et al*. 2018[17]) and named as "elimination of discontinuous velocities", can certainly increase the speed of the computer's processing in comparison with checking the force equilibrium at each time step. On the whole, the overall process for performing the proposed method is shown in Figure 2.

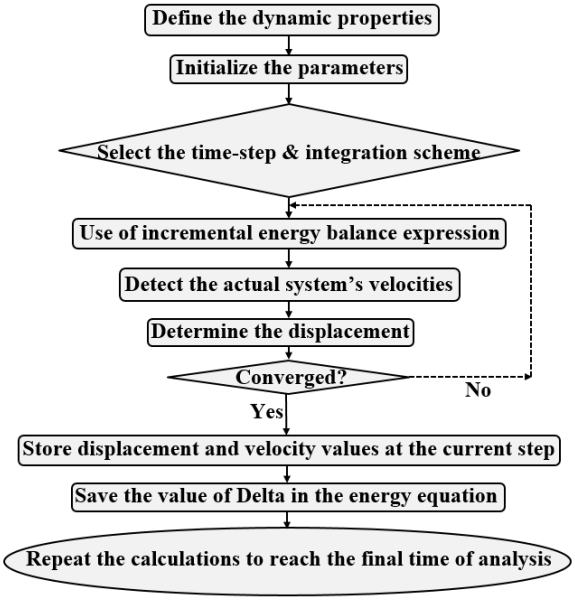

Fig. 2: Flowchart for implementing the proposed method

3.3. Generalizing the proposed method for nonlinear MDOF systems

A numerical method should be comprehensive, i.e., a method with fewer restrictions is more popular in practice. For this reason, after presenting the concepts of the modified energy method in the previous section for SDOF systems, here the presented technique will be demonstrated for MDOF structures with general nonlinear behavior. Now, we would like to consider an n-DOF structural system with the displacement vector $\mathbf{u}=[u_1,u_2,\ldots u_n]^T$. The matrix differential equation of motion, in this case, is assumed to be expressed as:

$$\mathbf{f_I}(\ddot{\mathbf{u}}) + \mathbf{f_D}(\dot{\mathbf{u}}) + \mathbf{f_S}(\mathbf{u}) = \mathbf{F}(t) \quad (24)$$

In Eq.(24), $\mathbf{f_D}$ and $\mathbf{f_S}$ respectively are two general nonlinear functions regarding velocity and displacement vectors; while, $\mathbf{f_I}$ and $\mathbf{F(t)}$ represent the inertial and external excitation force vectors.

By introducing the tangential damping, $\mathbf{c(t)}$, and stiffness, $\mathbf{k(t)}$, matrices; and, in a similar way for SDOF systems, the characteristic discretized equation as a function of velocities at the current time (t_{j+1}) is given by

$$A_i v_{i(j+1)}^2 + B_i v_{i(j+1)} + C_i = 0 \quad , \quad i = 1:n \tag{25}$$

where the subscript *i* denotes the number of DOF.
To avoid expressing the massive mathematical relations, the coefficients in the quadratic Eq.(25) along with the mathematical proof of how they are obtained are given in Appendix 1. Further, a step-by-step algorithm for computer implementation of the modified energy method (MEM) for a general nonlinear n-DOF system is provided in Table 3.

Table 3. Step-by-step algorithm for computer implementation of the modified energy method (MEM)

A) Inputs
1. Form mass **M**, damping **C(t)**, and stiffness **K(t)** matrices
2. Determine loading vector **F(t)** and duration of the analysis t_d
3. Select a time-step Δt and integration technique *r*
4. Impose the initial condition $\mathbf{u_0}$, $\mathbf{v_0}$
B) Preliminary calculation
5. Compute two integration constants; $a_1 = r\Delta t$, $a_2 = (1- r)\Delta t$
C) Step-by-step integration $t_j = j\Delta t$ (j=1,2,…, $t_d / \Delta t$)
6. Advance in the time domain; $t_{j+1} = t_j + \Delta t$
7. Form the velocity equations, regardless of the coupling terms; $A_i (v_{i(j+1)})^2 + B_i (v_{i(j+1)}) + C_i = 0$, i=1:n
8. Solve quadratic equations and detecting the actual system's velocities
9. Calculation of coupling terms and modification of coefficients in step 7
10. Repeat step 7 through 9 to achieve the convergence
11. Save the last calculated Delta of quadratic equations
12. Determine the displacement of the system in the current time using Euler's formula; $\mathbf{u}_{j+1} = \mathbf{u}_j + a_1.\mathbf{v}_{j+1} + a_2.\mathbf{v}_j$
13. Increase *j* and go to step 6 to reach the end of the analysis duration
D) Control of the calculations (determine the optimum time interval)
14. Stability control of the responses from the history of Delta and change the values of the parameters in step 3

3.4. Accuracy and Stability Analysis

This part deals with the analysis of the effect of choosing the size of the time step on the accuracy and stability of the proposed method. In this regard, according to (Bathe & Cimento 1980[2]; Bathe 2008[4]) these numerical features will be investigated through analyzing the free vibration response of a simple SDOF system shown in Figure 3.

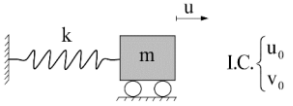

Fig. 3: A conservative mass-spring system to analyze the accuracy and stability of the numerical methods

3.4.1. Stability analysis of the proposed method

Regarding Figure 3, Eq.(18) can be simplified as below

$$\begin{cases} m\left[v_{j+1}^2 - v_j^2\right] + \Delta t\left[\not{c}_{j+1} v_{j+1}^2 + \not{c}_j v_j^2\right] + \underbrace{k_{j+1} u_{j+1}^2 - k_j u_j^2}_{k(u_{j+1}^2 - u_j^2)} \\ = \Delta t\left[\not{F}_{j+1} v_{j+1} + \not{F}_{j+1} v_j\right] \quad \text{(I)} \\ u_{j+1} = u_j + \Delta t\left[(1-r)v_j + (r)\, v_{j+1}\right] \quad \text{(II)} \end{cases} \tag{26}$$

Now by defining the two variables, $\lambda = \omega.\Delta t$ and $\beta = u_j / (\Delta t.v_j)$, one can combine these two equations as

$$(1 + r^2\lambda^2)v_{j+1}^2 + (v_j)(2r\lambda^2)(\eta + 1 - r)v_{j+1} + v_j^2(\lambda^2(1-r)^2 - 1 + 2\lambda^2(1-r)\eta) = 0 \tag{27}$$

As mentioned earlier, in order to avoid the creation of the imaginary velocities in the analysis, Delta in Eq.(27) must always have a non-negative value; that is,

$$\Delta(r, \lambda, \eta) \geq 0 \tag{28}$$

Utilizing the sign function (Sign) in this case can be useful in finding the stability region. So, by plotting the function of Sign(Δ) for three values of r=0, r=0.5, r=1 in Figure 4,5.

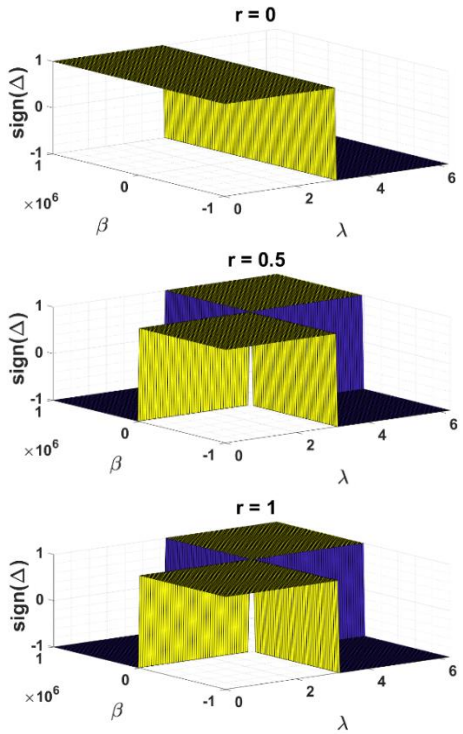

Fig. 4: The sign of Delta in the stability analysis of the proposed method

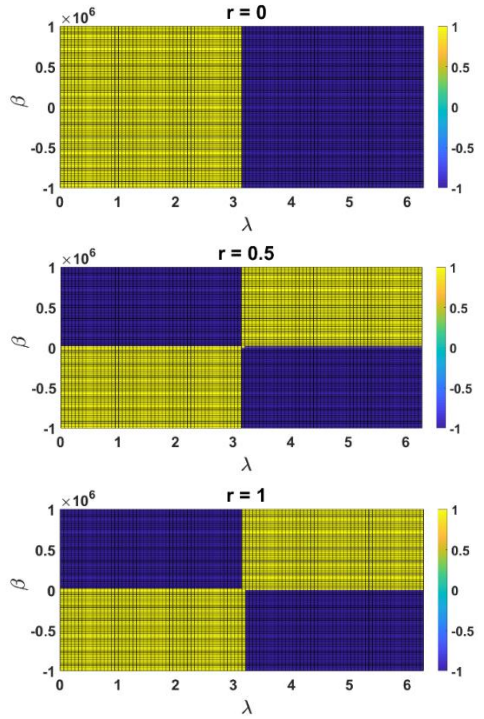

Fig. 5: Stability region in the λ-β plane

According to Figure 5, it can be seen that for the value of r = 0, the proposed method is stable regardless of the values of the β parameter. The stability condition in this case as a function of the natural period of the system, T, is given by

$$\omega\Delta t \le 3.2 \xrightarrow{\omega.T=2\pi} \frac{\Delta t}{T} \le \frac{3.2}{2\pi} \approx 0.509 \rightarrow \boxed{\Delta t_{cr} = 0.509\,T} \quad (29)$$

Moreover, for the other two modes (r = 0.5 and r = 1), which have a nearly sign function diagram, in contrast to the previous state (r = 0), where the stability region does not depend on the value of β, the positive sign of Delta cannot be guaranteed for a specified range of λ. As a result, it can be concluded from observing the results (for the three values for r) that the case r = 0 shows a more stable region and can be a better choice than the other two circumstances.

3.4.2. Accuracy analysis of the proposed method

According to an approach utilized in the literature (e.g., refer to (Bathe, 2014[3]) once again, the free-undamped response of a linear vibrating system (Figure 3) is employed in this study. In order to incorporate with unit values for the amplitude and period of vibration (A_{exact}=1, T_{exact}=1), the dynamical properties in the analysis are selected as below

$$m = 1, k = 4\pi^2, u_0 = 1, v_0 = 0 \quad (30)$$

As we know, the analytical or exact solution of this vibrational problem is u(t) = Cos2πt; while, the numerical response differs from this function, as shown in Figure 6 for three different values of r.

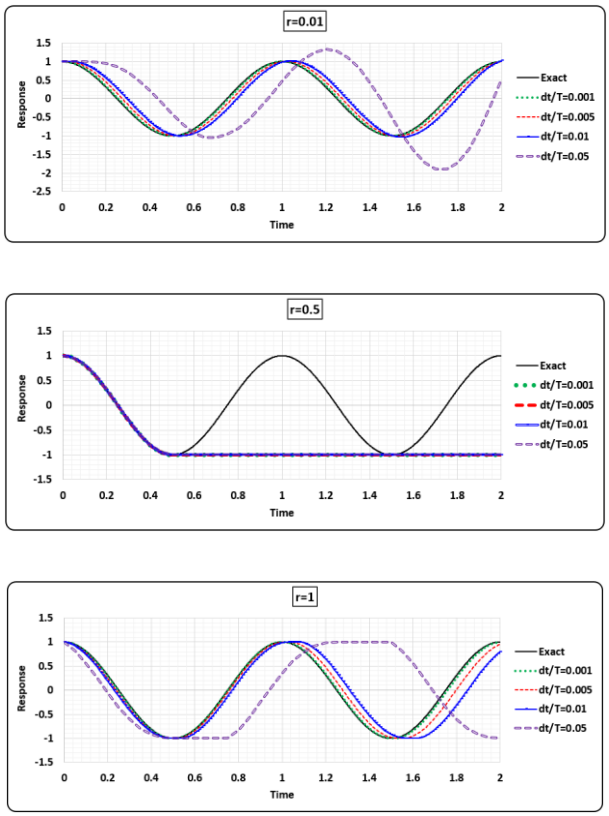

Fig. 6: Accuracy analysis of the proposed method for three value of r = 0, 0.5, 1

First, it should be noted that the value of r = 0.01 is chosen as the representative of the value of r = 0 (since otherwise, the method will not be self-started). The most important point that can be seen from Figure 6 is that the value of r = 0.01 has a better result than the other two cases. As an instance, for the values of r = 1 and especially r = 0.5, the calculated velocity of the numerical method has been zero in the significant range of the analysis period and has not changed, which does not correspond to the physical nature of a vibrational problem.

In the following, two relative parameters of the periodicity error (ε_T), as well as the amplitude error (ε_A), are defined to evaluate the accuracy.

$$\varepsilon_T = \left|\frac{T_{Num} - T_{Exact}}{T_{Exact}}\right| \xrightarrow{T_{Exact}=1} \boxed{\varepsilon_T(\%) = \left|T_{Num} - 1\right| \times 100}$$
$$\varepsilon_A = \left|\frac{A_{Num} - A_{Exact}}{A_{Exact}}\right| \xrightarrow{A_{Exact}=1} \boxed{\varepsilon_A(\%) = \left|A_{Num} - 1\right| \times 100} \quad (31)$$

In the above expressions, A_{Num} and T_{Num} (numerical amplitude and period) are functions of the selected time-step (Δt). According to Figure 7 for r = 0.01, the numerical errors of the method, including the percentage of amplitude and periodicity error, along with the

numerical damping, are compared with the 2nd order Range-Kutta method (RK2).

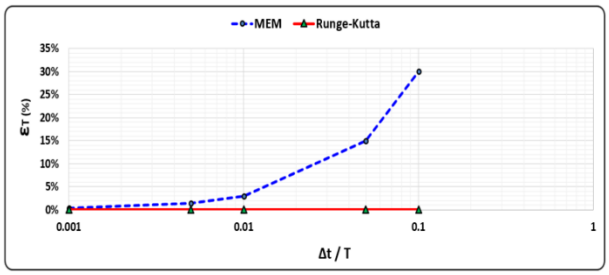

(a)

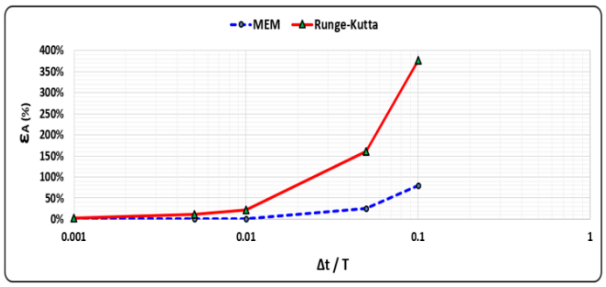

(b)

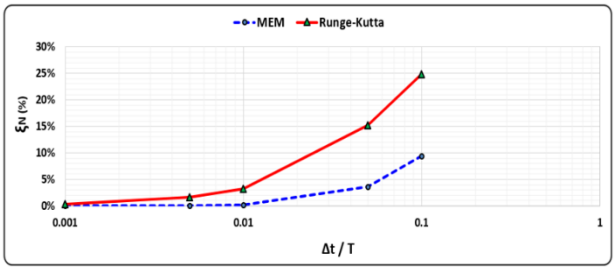

(c)

Fig. 7: The comparison between the accuracy of the presented method vs. 2nd Runge-Kutta technique: (a) periodicity error; (b) amplitude error; (c) numerical damping

As shown in Figure 7(a), the RK2 method does not have the periodicity error; nevertheless, the energy method produces the numerical error in the calculation of the vibrational period of the system as increasing the ratio of $\Delta t/T$. For example, for the ratios of $\Delta t/T$ = 0.01, 0.05, and 0.1 the value of these errors, respectively, are about 3, 15 and 30%. Furthermore, in Figure 7(b), the relative amplitude error is compared for two MEM and RK2 methods for different values of $\Delta t/T$. Contrary to the former case, it is observed that these errors in the vibrational amplitude are much lower than the RK2 method when using the energy method. Eventually, the percentages of artificial damping that the energy method produces in numerical analysis for different values of $\Delta t/T$ is compared to the RK2 method in Figure 7(c). Accordingly, for the ratio of $\Delta t/T$ = 0.1, the proposed method has introduced artificial damping of about 10% in the calculated response of the system, while this value for the RK2 method is nearly 25%.

4. Results and Discussion

In this section, some applicable examples in the structural and earthquake engineering are analyzed by the proposed numerical technique. The numerical results obtained by the presented method are compared with other conventional numerical approaches such as Newmark and Runge-Kutta techniques to reveal the computational aspects of this method. It shall be pointed out that all problems in this section have been implemented in the MATLAB environment.

4.1. A One-story building frame with elasto-plastic behavior under blast loading

As one of the most common nonlinear problems in earthquake engineering, an SDOF building model, according to Figure 8(a), is considered as the first example, taken from (Clough & Penzien 2013[10]). The system whose hysteretic behavior is elastic-perfectly plastic is subjected to a lateral blast loading as displayed in Figure 8(b). Other properties assumed in this problem are given in Table 4.

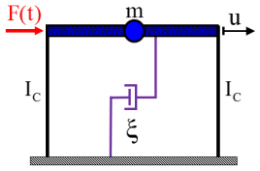

(a)

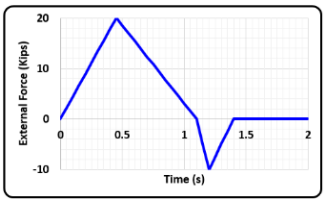

(b)

Fig. 8: A one-story building model: (a) configuration of the frame; (b) representation of lateral blast load

Table 4. The assumed properties for analyzing Example 4.1.

Type of parameters	Quantity	symbol	Value
System's characteristics	Mass	m	0.2 Kips.in^{-1}.s^2
	Viscous Damping ratio	ζ	8.7 %
	Elastic stiffness	k_1	12.35* Kips.in^{-1}
Loading	Blast load	$F(t)$	Figure 8(b)
Nonlinear behavior	post-yield to pre-yield stiffness	α	0
	Yield force	F_y	15 Kips
Analysis	Duration	t_d	2 s

*$24EI_C/L^3 = (24\times(3\times10^4)\times100)/(15\times12)^3$

For the problem at hand, the stiffness of the system, k_j, is not constant during the analysis. Based on Table 4, this parameter at time $t=t_j$, will take either one of the two

initial/elastic stiffness (k_1) or post-yielding stiffness (k_2) according to Eq.(32).

$$k_j = \begin{cases} k_2 & \text{if } \left|f_{s\,j}\right| \geq F_y \text{ and } df_{s\,j} > 0 \\ k_1 & \text{otherwise} \end{cases} \tag{32}$$

In this expression, the parameter $f_{S\,j}$ is the restoring force at time $t=t_j$, and the parameter $df_{S\,j}$ denotes the difference of this force for current and previous time steps; *i.e.*, $df_{S\,j} = \left|f_{S\,j}\right| - \left|f_{S\,(j-1)}\right|$. The remaining parameters are also defined in Table 4. Due to nonlinear nature of this problem, at each time step, the value of $f_{S\,j}$ is first estimated by the last calculated spring force ($f_{S\,j} \approx f_{S\,(j-1)}$), then it shall be refined by the values of k_j and u_{j+1} after computing the state of the system at time t_{j+1}.

For this example, in order to better familiarize the reader with the presented methodology, at first, the structure is analyzed with linear behavior (considering the elastic stiffness), and then an elastoplastic analysis is carried out. For the first case, in the beginning, to find the answer to the question, what values of the r parameter can have a closer response to the reference solution? Let us draw the results from the three values of r = 0, 0.5, 1 versus the linear response of the system in Figure 9. It is to be emphasized once again that according to Eq.(18) the presented method for such problems with the zero initial condition and F(0)=0 is not self-starting; so, to overcome to this issue a small value near zero (here, r=0.01) is utilized as a representative of the forward-Euler method (r=0). Note that the fourth-order Runge-Kutta along with Newmark (linear Acc.) methods are selected to obtain the reference solution of the system. In this situation, a very small size of time-step (i.e., $\Delta t = 10^{-4}$s) is used to ensure the approach entirely the numerical results to the exact solution of the system. It should be noted that the obtained response is also controlled with the linear response provided in Ref. (Clough & Penzien 2013[10]).

From Figure 9, it is proven that the mode r=0.01, which corresponds to the FE state, yields the best results in comparison with the other two cases (i.e., trapezoidal and BE modes).

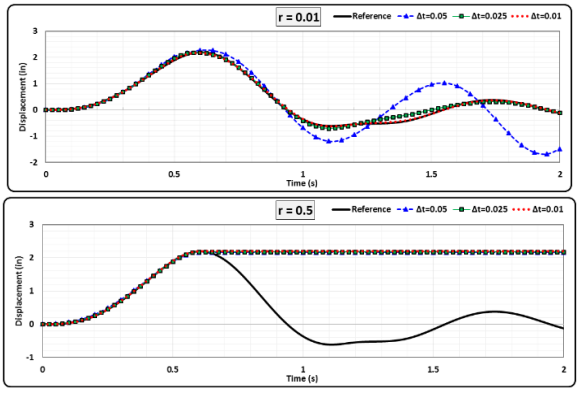

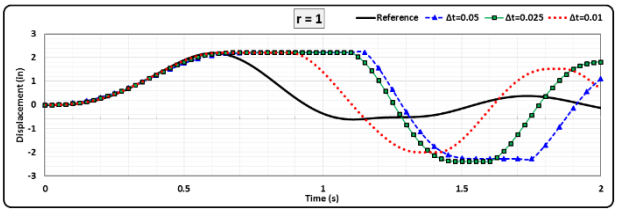

Fig. 9: The displacement response of the linear system for various values of parameters r and Δt

After estimating the proper value for r, to reveal one of the unique features of the proposed energy method, we will calculate the optimal time interval for the analysis. Indeed, with plotting the time history of the Delta parameter, to prevent the creation of the imaginary velocities in the analysis procedure, these graphs should lie above the horizontal axis of time. In this regard, the obtained results are depicted for the different values of Δt in Figure 10 for the case of the FE integration scheme.

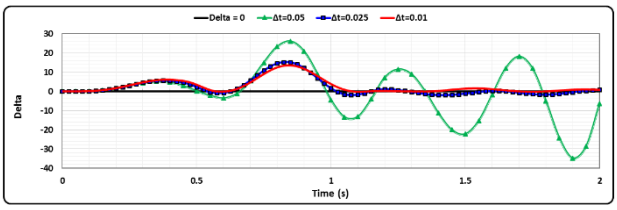

Fig. 10: The time-history of Delta in the case of r = 0 for different values of Δt in linear analysis

As expected, it can be seen from Figure 10 that by decreasing the size of the time interval with the upward movement of the curves, the negative values of the Delta parameter are vanishing. As for Δt = 0.01s, it can be almost ensured that the delta values are positive during the analysis; therefore, this value can be considered as the optimal time interval, Δt_{opt}.

Now, by performing the nonlinear analysis for this problem, the proper value for r for the case of elasto-plastic behavior can be obtained by testing three values for r respectively corresponding to FE, TR, and BE integrating schemes. In the nonlinear case, it is interesting to note that, the FE technique again is most consistent with the reference solution (which is obtained with a very small time-step ($\Delta t = 10^{-4}$s) by RK4 and Newmark methods). In this regard, the process of convergence of the numerical solution is shown in Figure 11 by decreasing the time-step interval for this model.

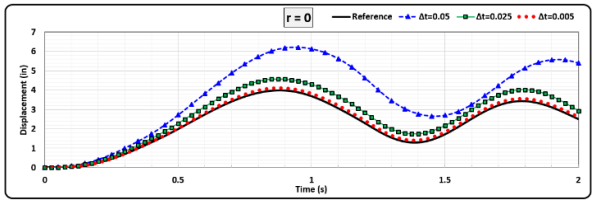

Fig. 11: The convergence process of the nonlinear time-history responses in Example 4.1 for r = 0.

In the following, in a similar way to the linear analysis, the optimum size of the time-step is selected as Δt = 0.005s for nonlinear analysis, and according to Figure 12.

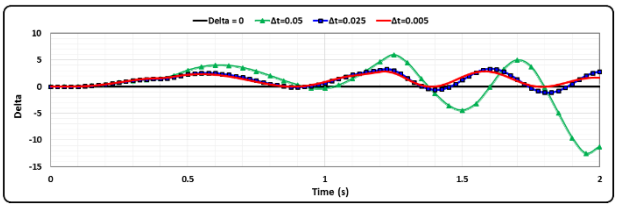

Fig. 12: The time-history of Delta in the case of $r = 0$ for different values of Δt in nonlinear analysis

After choosing the appropriate value of time-step for the analysis, the different results consist of the history of the displacement response, the force-deformation relationship, the phase-plane, and the energy history of the system can be depicted in Figure 13. The validation of these responses might be verified by RK4, Newmark, as well as (Clough & Penzien 2013[10]).

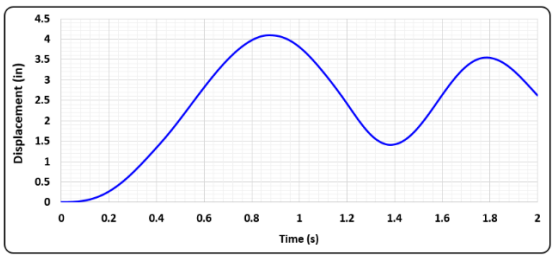

(a)

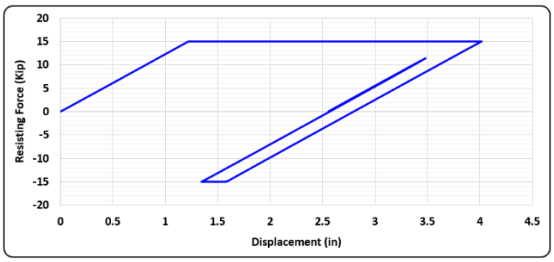

(b)

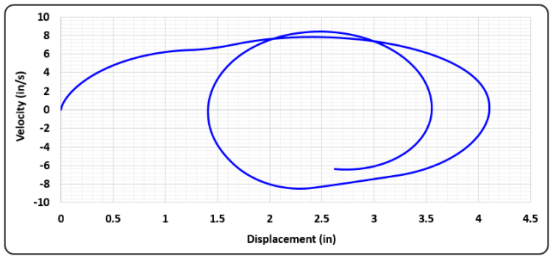

(c)

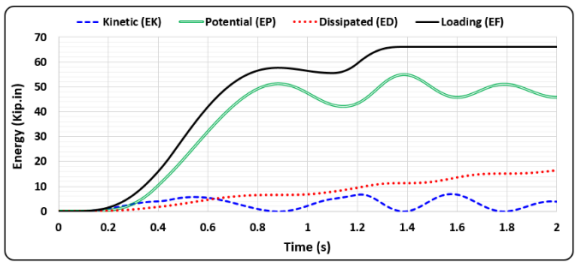

(d)

Fig. 13: The nonlinear response of elasto-plastics system: (a) time-history of displacement; (b) force-deformation diagram; (c) phase-plane; (d) time-history of energies

4.2. The vibration of a shape-memory alloy (SMA) subjected to harmonic loading

Recently, the SMA materials due to their super-elastic behavior are highly regarded for improving the seismic performance of structures in earthquake engineering (Mahmoudi *et al*. 2018[24]). Although, in practice, few software can analyze the hysteretic behavior of this type of material directly. In this way, the combination of two elastic and plastic systems or modification of some models such as MPF (Mazzoni *et al*. 2007[25]) in Openness software is often used for practical applications. Here, an SMA oscillator with zero initial conditions is considered by Table 5, for analyzing by MEM. To better illustrate the material nonlinearity for the problem at hand, the skeleton curve of hysteretic behavior is illustrated in Figure 14.

Table 5. The properties for analyzing Example 4.2

Type of parameters	Quantity	symbol	Value
System's characteristics	Mass	m	1 N.mm^{-1}.s^2
	Damping ratio	ζ	10 %
	Initial stiffness	k_1	1 N.mm^{-1}
Loading (Cosine)	Excitation frequency	Ω	4 Rad.s^{-1}
	Amplitude of load	P_0	200 N
Nonlinear behavior	Plastic/Elastic stiffness	α	0.1
	Yield force	F_A	4 N
	The force in unloading at $k_1 \rightarrow k_2$	F_C	4 N
Analysis	Duration	t_d	3.5 s

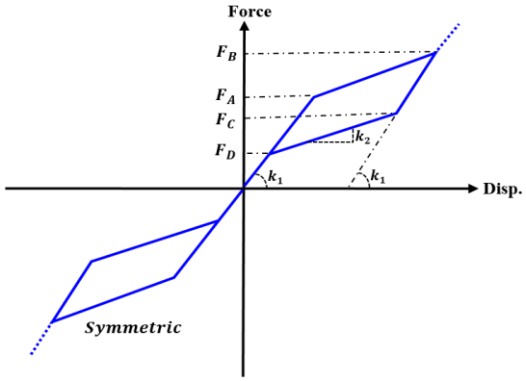

Fig. 14: The nonlinear Force-Disp. behavior

In this problem, the instantaneous stiffness, k_j (at time t_j) can be defined as

$$k_j = \begin{cases} k_2 & \left(if \;\; F_A < \left|f_{S\,j}\right| < F_B \;\; and \;\; df_{S\,j} > 0\right) \\ & or \;\; \left(if \;\; F_D < \left|f_{S\,j}\right| < F_C \;\; and \;\; df_{S\,j} < 0\right) \\ k_1 & otherwise \end{cases} \quad (33)$$

In this case, for the verification of the numerical solutions obtained by the energy method, the RK4 and Newmark are employed as the reference solution with a tiny time step (Δt=0.0001s) to ensure that the numerical solution approaches the exact solution of the problem. Herein, to select the appropriate value for the parameter r, using three values of Δt = 0.1s, 0.05s and 0.01s, the time-history of displacement is plotted for three different values of r = 0, 0.5, 1 according to Figure 15.

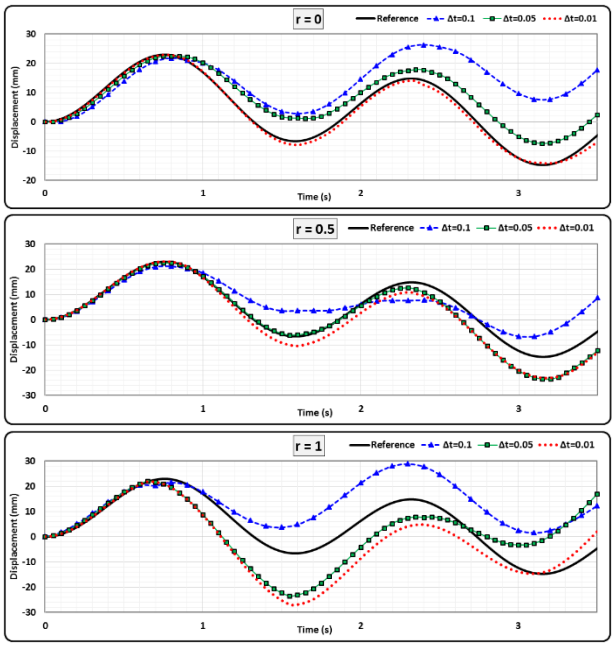

Fig. 15: The displacement response of the system for various values of parameters r and Δt

According to the above diagrams, it can be seen that the case of r = 0, among the three values chosen for r, has better results when the results are compared with the reference solution. Hence, by fixing this value for the analysis, the optimum value of the time interval (Δt_{opt}), can be determined by utilizing the time-history of the Delta, as shown in Figure 16.

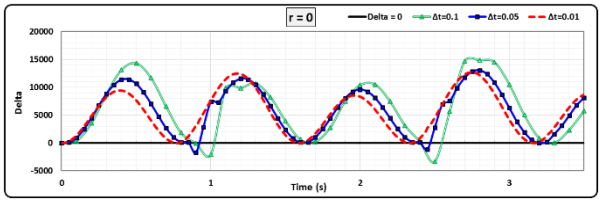

Fig. 16: The time-history of Delta in the case of r = 0 for different values of Δt

Based on the results observed from Figure 16, as expected, by decreasing the size of time-steps, the graphs move upward, and the negative values are reduced. Therefore, in order to avoid creating imaginary velocities in the analysis of this problem, the value of Δt = 0.01s seems to be appropriate. So, the numerical solutions correspond to this value, including the displacement history and phase-plane, along with the history of mechanical energies are plotted in Figure 17.

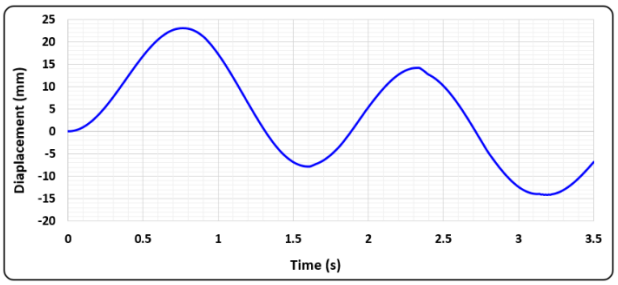

(a)

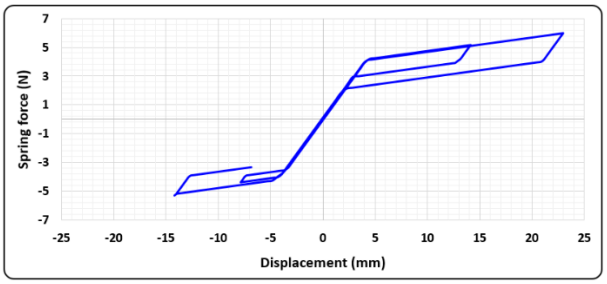

(b)

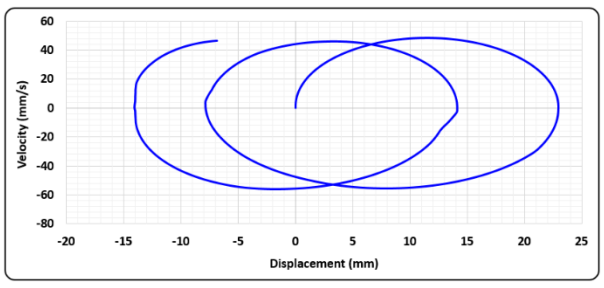

(c)

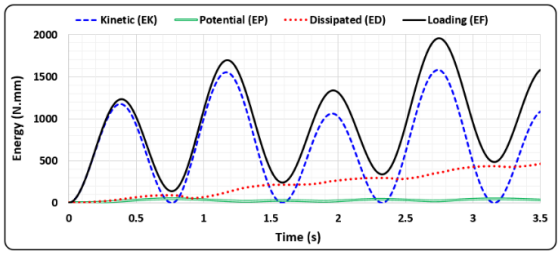

(d)

Fig. 17: The nonlinear response of elasto-plastics system: (a) time-history of displacement; (b) force-deformation diagram; (c) phase-plane; (d) time-history of energies

4.3. A beam with compatible mass and non-classical damping matrices vibrating under a unit step load

A beam element with two DOF including the translation, u_1, and rotation, u_2, is considered as shown in Figure 18.

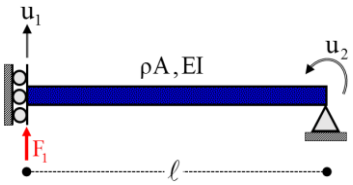

(a)

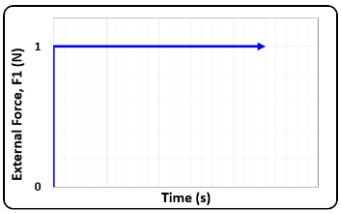

(b)

Fig. 18: Vibrating beam structure: (a) beam element characteristics; (b) applied step load

According to (Weaver & Johnston 1987[34]) and using the concept of shape-functions in the finite element method, the mass (**m**) and stiffness (**k**) matrices for this structure can be expressed by

$$\mathbf{m} = \frac{\rho A \ell}{420}\begin{bmatrix} 156 & -13\ell \\ -13\ell & 4\ell^2 \end{bmatrix} \quad , \quad \mathbf{k} = \frac{2EI}{\ell^3}\begin{bmatrix} 6 & 3\ell \\ 3\ell & 2\ell^2 \end{bmatrix} \tag{34}$$

For simplifying the calculation of the analytical solution of this problem, by assuming the numeric parameters as beam's length (ℓ=1m), mass per unit length (ρA=420kg/m), and flexural rigidity (EI=21.87N.m^2). The first and second undamped natural frequencies of this vibrating system would be equal to T_1=11.11sec and T_2=1sec. If we want to construct a proportional damping matrix (based on the Rayleigh damping), by assuming a damping ratio of 5% for both of the first and second modes, the damping matric would be written as **c**=[11.91 , 1.24; 1.24 , 1.48]; but, in order to have a general damping matrix, a non-classical/non-proportional damping matrix are used for the analysis. Overall, in this case, the governing equation of motion can be expressed in the following matrix form.

$$\begin{bmatrix} 156 & -13 \\ -13 & 4 \end{bmatrix}\begin{bmatrix} \ddot{u}_1 \\ \ddot{u}_2 \end{bmatrix} + \begin{bmatrix} 10 & 2 \\ 2 & 4 \end{bmatrix}\begin{bmatrix} \dot{u}_1 \\ \dot{u}_2 \end{bmatrix} + \begin{bmatrix} 262.44 & 131.22 \\ 131.22 & 87.48 \end{bmatrix}\begin{bmatrix} u_1 \\ u_2 \end{bmatrix} = \begin{bmatrix} H(t) \\ 0 \end{bmatrix} \tag{35}$$

As we know, in this case, the conventional modal analysis cannot be used directly since the damping matrix is not proportional, and complex normal modes must be used to obtain the exact solution of the system. Moreover, due to the existence of non-diagonal terms in the mass matrix, these second-order differential equations cannot be expressed in the state-space form; so, the Runge-Kutta techniques are also not applicable to this problem. Here, the Laplace transform is employed to obtain the exact response of the system as below (for interested readers a detailed mathematical proof is provided in Appendix 2).

$$\begin{cases} u_1 = 0.0152 + 0.000091\exp(-0.7539t)\cos(6.2362t - 3.3387) \\ +0.01516\exp(-0.0328t)\cos(0.5644t - 3.0874) \\ u_2 = -0.0228 + 0.00092\exp(-0.7539t)\cos(6.2362t - 3.2823) \\ +0.02382\exp(-0.0328t)\cos(0.5644t - 0.0670) \end{cases} \tag{36}$$

To solve this 2-DOF system using the MEM, as described in Section 3.3, by decomposing the mass, damping, and stiffness matrices into two diagonal and non-diagonal matrices, the displacement history and the rotation of the beam can be computed by a computer program by means of Table 3. Once again, among three values of r=0, 0.5, 1, the first one, which has a better agreement with the exact/reference solution is shown in Figure 19.

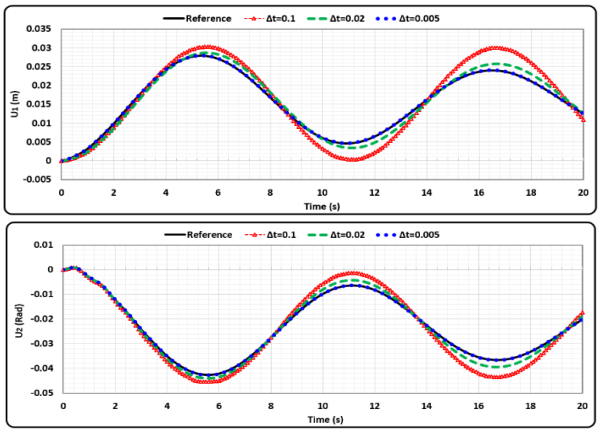

Fig. 19: The convergence process of the nonlinear time-history responses in Example 4.3 for r = 0: (a) translation DOF, u$_1$; (b) rotational DOF, u2

In order to choose the optimum value of Δt, once again, we can monitor the time-history of Delta for the various value of time intervals. Obviously, there is more than one

Delta for these MDOF systems. For example, in the example above, we can draw two histories of the Delta parameter for the first and second DOFs, as shown in Figure 20. In these conditions, to choose the optimal size of the time interval, the most critical (negative) amount is used among all the cases.

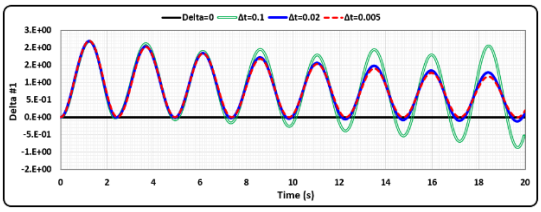

(a)

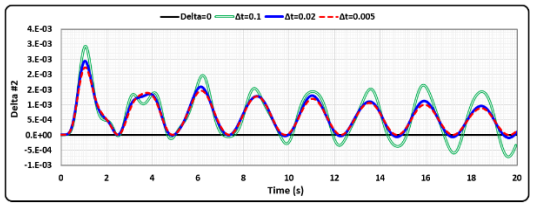

(b)

Fig. 20: Time-history of Delta:
(a) translation DOF, u_1; (b) rotational DOF, u2

With respect to both graphs from Figure 20, it is observed that the value of Δt = 0.02s can be almost a proper choice to take for the optimum time-step. Nevertheless, from a more conservative point of view, the value of Δt = 0.005s that leads to a more positive value for both translation and rotational DOFs for Delta in the whole time of analysis is utilized as an optimal size for time-step for this problem.

In the following, the numerical results correspond to Δt = 0.005s, including the displacement history and phase-plane along with the history of mechanical energies are plotted in Figure 21. It is to be noted that the validity of these results is verified with the closed-form solution by Eq.(36).

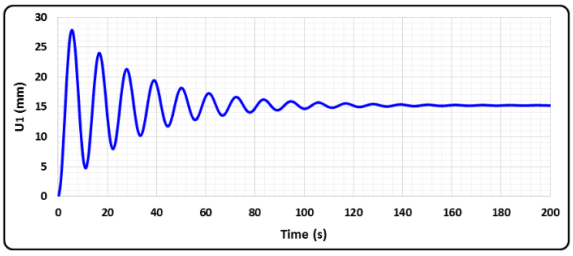

(a)

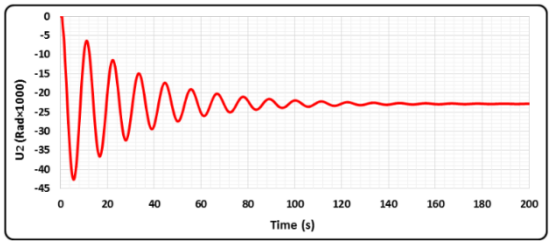

(b)

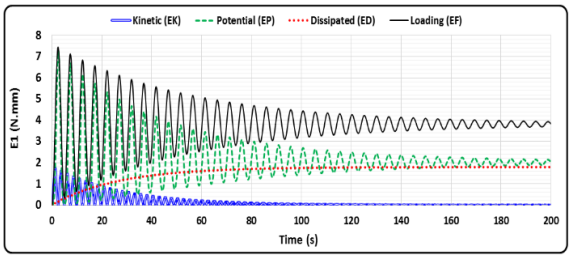

(c)

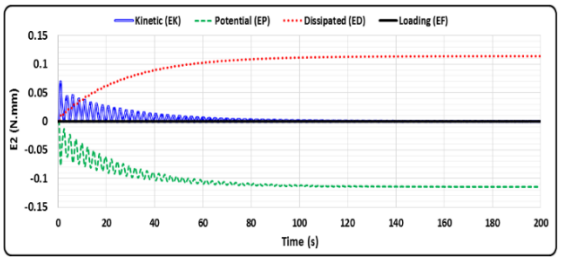

(d)

Fig. 21: Time-history of different responses:
(a) DOF#1,u_1; (b) DOF#2, u_2; (c) energy of the first DOF, E_1; (d) energy of the second DOF, E_2

By observing Figures 21(a) and (b), it can be seen that the dynamic responses ($u_1(t)$, $u_2(t)$) after time-lapse (reaching the steady-state condition) will approaches to their corresponding static values; i.e., $u_{1st} = \ell^3/3EI$ = 0.0152 *m* and $u_{2st} = \ell^2/2EI$ = – 0.0228 *Rad*). These values can further be applicable in verifying the Eq.(36) as the time approaches the infinity and the vanishing of the exponential terms when $t \to \infty$. Furthermore, Figures 21(c) and (d) are also demonstrate the energy equilibrium of the system during the analysis; that is, the summation of kinetic, dissipated, and potential energies at any instant are equal to the external energy applied by the loading on the system.

4.4. Seismic analysis of a multi-story building frame with nonlinear behavior

A 3-story building frame as shown in Figure 22(a) with dynamic characteristics, according to Table 6, will be analyzed in this example.

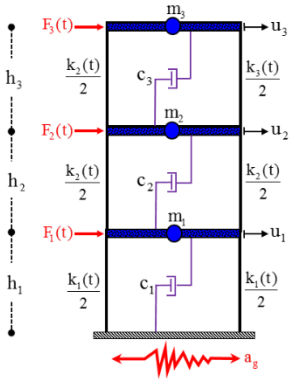

(a)

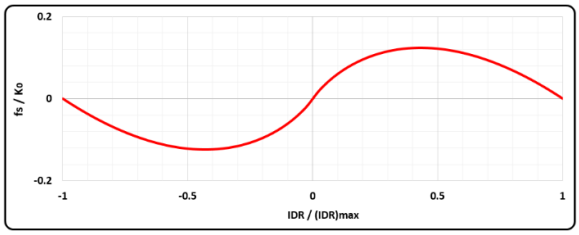

(b)

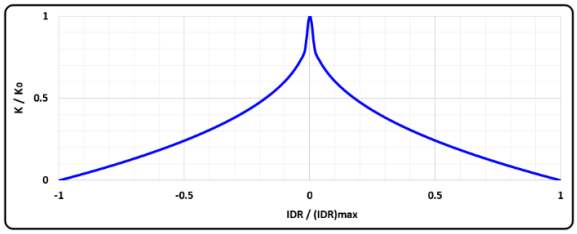

(c)

Fig. 22: (a) 3-story building under seismic load; (b) tangential inter-story stiffness (c) nonlinear column forces.

Table 6. The assumed properties for analyzing Example 4.4.

parameters	Quantity	symbol	Value
System's characteristics	Roof's masses	$m_1=m_2=m_3$	1 Ton.m^{-1}.s^2
	Damping coefficients	$c_1=c_2=c_3$	0.628 Ton.m^{-1}.s
	Initial inter-story stiffness	$k_1(0)= k_2(0)=k_3(0)$	10 Ton.m^{-1}
Loading	Earthquake	a_g	Loma
Analysis	Duration	t_d	2 s

For the current problem, the horizontal ground motion of the Loma earthquake (scaled to 0.35g) is considered as the external excitation. Also, herein it is assumed the resisting force of columns is a nonlinear function of the inter-story displacement, as depicted in Figure 22(b). In this case, the instantaneous inter-story stiffness, $k(t)$, from Figure 22(c) can be expressed regarding the initial stiffness, k_0, and the inter-story drift ratio (IDR) as follows.

$$k_i(t) = k_{0i}(1 + q_i \left| IDR_i \right|^n) \tag{37}$$

In the above equation, the subscript i specifies the story number; the coefficient q also corresponds to linear behavior for a value of zero, and its positive and negative values represent the hardening and softening behavior in the system, respectively. In this research, the value of 0.2 is selected for the power of n, according to (Chang *et al*. 2017[7]). In addition, the coefficient q is assumed to be the same for all three resisting force of columns; so, by assuming a softening behavior, the value of q=-2.65 is used by performing a trial and error process based on the absence of negative stiffness in any of the stories (in this regard, see Figure 23).

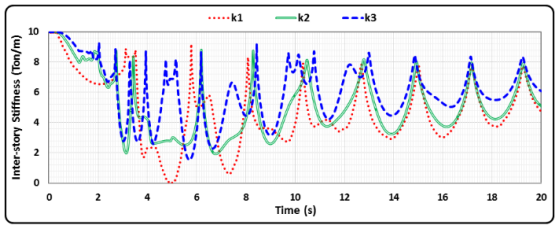

Fig. 23: The variation of the stiffness of stories vs. time

In the following, as an instance, the bottom floor displacement response of the system is obtained by MEM. The results are compared with those of Newmark and RK2 in Figure 24(a). Overall, from this graph, it can be seen that the result in the case of r=0 has good agreement these two well-known numerical techniques; while, in the case of r=0.5 and r=1 have not been able to produce accurate results, and they are very different from the response given by the Newmark and RK2. The restoring force against the displacement of the 1st floor is also plotted in Figure 24(b).

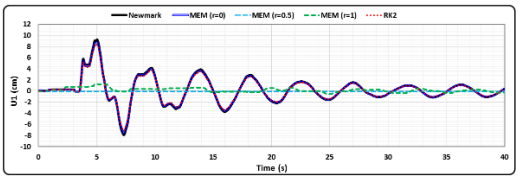

(a)

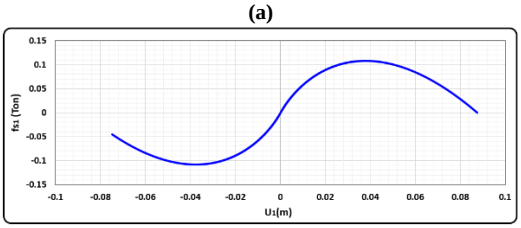

(b)

Fig. 24: The nonlinear response of the first floor: (a) time-history of displacement; (b) restoring force

Similar to the former example, we can plot the time-history of Delta in order to find the information about the precision of the obtained solution, as displayed in Figure 25. In this case, the size of time steps is fixed (Δt=0.005s), and we cannot decrease them to ensure the positive Delta parameters in each story. However, according to this diagram, it is observed that the values of Delta in all of the stories almost remain positive during the analysis, which is in line with the findings of Figure 24(a).

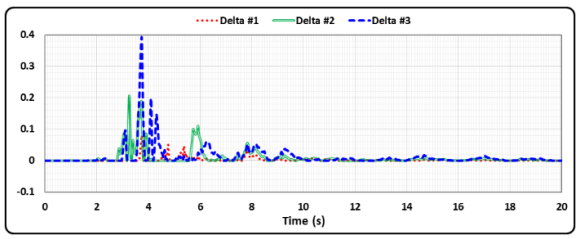

Fig. 25: The variation of Delta for all of three stories

Finally, a question that may arise in the mind of the reader is whether the proposed method can be applied to the dynamic analysis of geometrically nonlinear frame-like structures? To this end, the following describes how to apply the proposed computational scheme to these problems, and then gives a numerical example in this regard. As we know in nonlinear geometric problems, the stiffness matrix is a function of the displacements of the system. For instance, the stiffness matrix for a six-DOF frame element with geometric nonlinearity is derived in Appendix 3. In these cases, after assembling the local stiffness matrices, the global stiffness matrix of the structure is obtained as $\mathbf{K}(\boldsymbol{u})$. For simplicity in numerical computations, this matrix is usually expressed as the sum of two separate matrices $\mathbf{K}(\boldsymbol{u})=\mathbf{K}^{e}+\mathbf{K}^{g}(\boldsymbol{u})$; one elastic matrices, $\mathbf{K}^{e}$, plus a geometric stiffness matrix, $\mathbf{K}^{g}(\boldsymbol{u})$, (where arrays are a function of the current geometry of the system). To implement the presented approach in these cases, it will suffice to update the $\mathbf{K}^{g}(\boldsymbol{u})$ matrix (after calculating structural displacements) during each time step.

4.5. Dynamic response of an arch with large deflection under time-varying pressure

A circular shallow arc with the geometry shown in Figure 26 subjected to a dynamic pressure loading, depicted in Figure 27, will be analyzed here. This is an example of geometrically nonlinear problems in which material behavior is considered to be elastic.

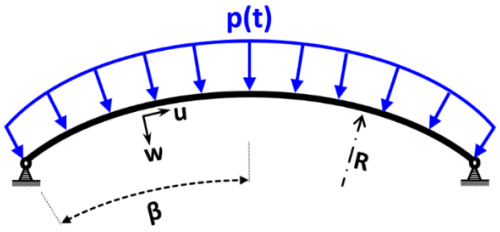

Fig. 26: A view of the arch structure

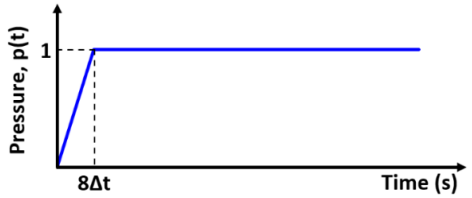

Fig. 27: Time variation of the uniform pressure loading.

The dynamical response of this system was first studied by Humphreys (1966[15]) using the Galerkin approximation, and then other researchers such as (Wilson *et al*. 1972[36]) implemented their proposed time integration method on it. The parameters related to this problem are listed in Table 7 in accordance with the above references.

Table 7. Dynamic data used for analyzing Example 4.5

Type of parameters	Quantity	symbol	Value
Arch geometry	Half of the subtended angle	β	**30** Degree
	Thickness	h	**2** in
	Arch radius	R	**73** in
Material Properties	Mass density	ρ	**6.25×10^{-3}** lb_m/in^3
	Elastic modulus	E	**3326** Psi
Analysis	Duration	t_d	**1.5** s

To implement the proposed method to the problem at hand, first, the arc shape of the structural geometry is approximated with straight segments. In this regard, ten frame elements have been selected by performing the sensitivity analysis and also the trial and error process on the number of these components. Accordingly, by ignoring the damping effects, and by forming the mass and stiffness matrix of these elements (see Appendix 3) and then the nodal load vectors, with assembling the local matrices in global coordinates of the structure, the equilibrium equations are solved by the MEM. It is noteworthy that, given the multiplicity of DOF in this structural system, parameter $\bar{\Delta}$ is defined as the ratio of average transverse displacements to the mean arch rise as follows.

$$\bar{\Delta}(t)=\frac{\frac{1}{L}\int_{0}^{L} w(x,t)}{\frac{1}{L}\int_{0}^{L} y_{0}(x)}=\frac{\int_{0}^{L} w(x,t)}{\frac{H}{2}} \tag{38}$$

In Eq.(38), $w(x,t)$ is the transverse deflection along the arch; $y_0(x)$ represents the initial quadratic shape of the structure; H and L also stand for arch rise and length, respectively.

To validate the numerical results obtained by the MEM, the time-history response presented by (Wilson *et al*. 1972[36]) is selected as the reference solution. In this way, three time-steps Δt=0.02s, Δt=0.01s, and Δt=0.005s are used according to Figure 28. It can be seen from this graph that as time steps become smaller, the numerical results of the energy method converge well to the reference solution.

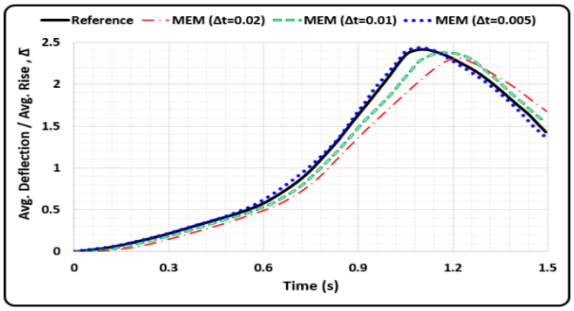

Fig. 28: Time-history responses of the energy method for three values of time intervals versus reference solution.

5. Conclusion

In the present research, a new form of the Modified Energy Methods (MEM) is introduced to numerically analyze the time-dependent response of general nonlinear structures. In this technique, the analyst rather than dealing with three unknowns (acceleration, velocity, and displacement) encounters only with velocity and displacement during a time-history analysis.

The stability analysis of the method showed that in a linear finite element system with the smallest period of T_n, in the case of r=0, the critical value of time-step is equal to $\Delta t_{cr}=0.509T_n$; while, for other values of the parameter r (i.e., r = 0.5, 1), the stability condition cannot be guaranteed for a specific range of Δt. According to the previous result, by choosing the value of r = 0 (Euler's Forward integration method), the accuracy analysis also indicated that the RK2 technique possesses much larger amplitude and artificial damping errors compared to the MEM. Moreover, regarding the selection of additional parameters for the direct time integration methods, the presented form only requires to define a parameter r where the results of Section 4 overall showed that the value of r = 0 (or values close to zero) is appropriate to compute the dynamic response of structures, accurately. Besides, the quadratic form of the discrete equations in terms of system's velocities creates a unique feature in the method, which is absent in any of the existing methods in the dynamic analysis of structures; that is, based on the assumption of avoiding the creation of imaginary velocities in the analysis process, an additional condition can provide useful information to the analyst in terms of controlling the selected size of time interval, especially in nonlinear analyzes. By the other words, in this technique, unlike conventional methods, the optimal size of the time-steps interval in the analysis is a function of external loading and in particular the nonlinear properties of the model used in the analysis.

Performing a dynamic analysis with the variable time intervals using the modified energy method is a desirable subject for future work. Besides, more research is needed to apply and test the presented idea to the analysis of equations of the system of other complex systems in engineering, such as dam-reservoir equations.

References

[1] Bathe, K.J., "Conserving energy and momentum in nonlinear dynamics: A simple implicit time integration scheme", Computers and Structures, vol. 85(7-8), 2007, p. 437–445.

[2] Bathe, K.J., Cimento, A.P., "Some practical procedures for the solution of nonlinear finite element equations", Computer Methods in Applied Mechanics and Engineering, vol. 22(1), 1980, p. 59–85.

[3] Bathe, K.J., "Finite element procedures", Prentice Hall, Pearson Education, 2014.

[4] Bathe, K.J., "On finite element methods for nonlinear dynamic response", In 7th European Conference on Structural Dynamics, 2008, p. 1239–1244.

[5] Bayat, M., Pakar, I., Bayat, M., "High conservative nonlinear vibration equations by means of energy balance method", Earthquakes and Structures, vol. 11(1), 2016, p. 129–140.

[6] Belytschko, T., Kam, W., Moran, B., Elkhodary, K.I., "Nonlinear Finite Elements for Continua and Structures", 2014.

[7] Chang, S.Y., Tran, N.C., Wu, T.H., Yang, Y.S., "A One-Parameter Controlled Dissipative Unconditionally Stable Explicit Algorithm for Time History Analysis". Scientia Iranica, 2017.

[8] Chung, J., Hulbert, G.M., "A time integration algorithm for structural dynamics with improved numerical dissipation: the generalized-α method", Journal of Applied Mechanics, vol. 60(2), 1993, p. 371–375.

[9] Cilsalar, H., Aydin, K., "Parabolic and cubic acceleration time integration schemes for nonlinear structural dynamics problems using the method of weighted residuals", Mechanics of Advanced Materials and Structures, vol. 23(7), 2016, p. 727–738.

[10] Clough, R., Penzien, J., "Dynamics of Structures", Berkeley, California, USA: Computers and Structures, 2013.

[11] Farhat, C., Chapman, T., Avery, P., "Structure-preserving, stability, and accuracy properties of the energy-conserving sampling and weighting method for the hyper reduction of nonlinear finite element dynamic models", International journal for numerical methods in engineering, (March), 2015, p. 1885–1891.

[12] He, J., "Preliminary report on the energy balance for nonlinear oscillations", Mechanics Research Communications, vol.29(2-3), 2002, p. 107–111.

[13] Hilber, H.M., Hughes, T.J.R., Taylor, R.L., "Improved numerical dissipation for time integration algorithms in structural dynamics", Earthquake Engineering & Structural Dynamics, vol. 5(3), 1997, p. 283–292.

[14] Houbolt, J.C., "A recurrence matrix solution for the dynamic response of elastic aircraft", Journal of the Aeronautical Sciences, vol. 17(9), 1950, p. 540–550.

[15] Humphreys, J.S., "On dynamic snap buckling of shallow arches", AIAA journal, vol. 4(5), 1966, p.878–886.

[16] Jalili Sadr Abad, M., Mahmoudi, M., Dowell, E.H., "Dynamic Analysis of SDOF Systems Using Modified Energy Method", Asian journal of civil engineering (BHRC), vol.18(7), 2017, p. 1125–1146.

[17] Jalili Sadr Abad, M., Mahmoudi, M., Dowell, E.H., "Novel Technique for Dynamic Analysis of Shear-Frames Based on Energy Balance Equations", Scientia Iranica, 2018, p. 1–31.
[18] Khan, Y., Mirzabeigy, A., "Improved accuracy of He's energy balance method for analysis of conservative nonlinear oscillator", Neural Computing and Applications, vol. 25(3-4), 2014, p. 889–895.
[19] Kim, W., "Improved Time Integration Algorithms for the Analysis of Structural Dynamics", 2016.
[20] Kim, W., Choi, S.Y., "An improved implicit time integration algorithm: The generalized composite time integration algorithm", Computers & Structures, vol. 196, 2018, p. 341–354.
[21] Kolay, C., Ricles, J.M., "Development of a family of unconditionally stable explicit direct integration algorithms with controllable numerical energy dissipation", Earthquake Engineering & Structural Dynamics, vol. 43(9), 2014, p. 1361–1380.
[22] Kolay, C., Ricles, J.M., "Assessment of explicit and semi-explicit classes of model-based algorithms for direct integration in structural dynamics", International Journal for Numerical Methods in Engineering, vol. 107(1), 2016, p. 49–73.
[23] Kuhl, D., Crisfield, M.A., "Energy-conserving and decaying algorithms in non-linear structural dynamics", International Journal for Numerical Methods in Engineering, vol. 45(November 1997), 1999, p. 569–599.
[24] Mahmoudi, M., Montazeri, S., Jalili Sadr Abad, M., "Seismic performance of steel X-knee-braced frames equipped with shape memory alloy bars", Journal of Constructional Steel Research, vol. 147, 2018, p. 171–186.
[25] Mazzoni, S., Mckenna, F., Scott, M.H., Fenves, G.L., "OpenSees Command Language Manual", 2007.
[26] Navarro, H.A., Cveticanin, L., "Amplitude-frequency relationship obtained using Hamiltonian approach for oscillators with sum of non-integer order nonlinearities", Applied Mathematics and Computation, vol. 291, 2016, p. 162–171.
[27] Newmark, N.M., "A method of computation for structural dynamics", Journal of the Engineering Mechanics Division, vol. 85(3), 1959, p. 67–94.
[28] Park, K.C., "An improved stiffly stable method for direct integration of nonlinear structural dynamic equations", J. Appliled Mechanics, Trans. ASME, vol. 42(2), 1975, p. 464–470.
[29] Razzak, M.A., Rahman, M.M., "Application of new novel energy balance method to strongly nonlinear oscillator systems", Results in Physics, vol. 5, 2015, p. 304–308.
[30] Reddy, J.N., "An Introduction to Nonlinear Finite Element Analysis: with applications to heat transfer, fluid mechanics, and solid mechanics", OUP Oxford, 2014.
[31] Rostami, S., Shojaee, S., Moeinadini, A., "A parabolic acceleration time integration method for structural dynamics using quartic B-spline functions", Applied Mathematical Modelling, vol. 36(11), 2012, p. 5162–5182.
[32] Shojaee, S., Rostami, S., Abbasi, A., "An unconditionally stable implicit time integration algorithm : Modified quartic B-spline method", computers and structures, vol. 153, 2015, p. 98–111.
[33] Soroushian, A., "Integration Step Size and its Adequate Selection in Analysis of Structural Systems Against Earthquakes", In Computational Methods in Earthquake Engineering, Springer, 2017, p. 285–328.
[34] Weaver J.W., Johnston, P.R., "Structural dynamics by finite elements", Prentice-Hall Englewood Cliffs (NJ), 1987.
[35] Wen, W.B., Wei, K., Lei, H.S., Duan, S.Y., Fang, D.N., "A novel sub-step composite implicit time integration scheme for structural dynamics", Computers & Structures, vol. 182, 2017, p. 176–186.
[36] Wilson, E.L., Farhoomand, I., Bathe, K.J., Nonlinear dynamic analysis of complex structures. Earthquake Engineering & Structural Dynamics, 1(March 1972), 1973, p. 241–252.
[37] Zhang, L., Liu, T., Li, Q., "A Robust and Efficient Composite Time Integration Algorithm for Nonlinear Structural Dynamic Analysis", 2015.
[38] Zienkiewicz, O.C., Taylor, R.L., Fox, D., "The Finite Element Method for Solid and Structural Mechanics", 2014.

Appendices

Appendix 1. Mathematical Proof of the MEM for General Nonlinear MDOF Systems

By focusing on the i[th] row in Eq.(24), one can write

$$\begin{aligned} &m_{i1}\ddot{u}_1 + \cdots + m_{ii}\ddot{u}_i + \cdots + m_{in}\ddot{u}_n + \\ &c_{i1}(t)\dot{u}_1 + \cdots + c_{ii}(t)\dot{u}_i + \cdots + c_{in}(t)\dot{u}_n + \\ &k_{i1}(t)u_1 + \cdots + k_{ii}(t)u_i + \cdots + k_{in}(t)u_n = F_i \end{aligned} \tag{A.1}$$

Multiplying by du_i and integrating from t_j to t_{j+1}, gives

$$\begin{aligned} &\int [m_{i1}\ddot{u}_1 + \cdots + m_{ii}\ddot{u}_i + \cdots + m_{in}\ddot{u}_n]\,du_i + \\ &\int [c_{i1}(t)\dot{u}_1 + \cdots + c_{ii}(t)\dot{u}_i + \cdots + c_{in}(t)\dot{u}_n]\,du_i + \\ &\int [k_{i1}(t)u_1 + \cdots + k_{ii}(t)u_i + \cdots + k_{in}(t)u_n]\,du_i = \int F_i\,du_i \end{aligned} \tag{A.2}$$

According to the presented context in Section 3.1, each part of this expression can be expressed as the change of one type of mechanical energy. For example, the variation of the kinetic energy

$$\begin{aligned} \Delta E_{Ki} &= \frac{1}{2}m_{ii}v_{i(j+1)}^2 - \frac{1}{2}m_{ii}v_{i(j)}^2 + \\ &\sum_{\ell=1,\neq i}^{n} [m_{i\ell}\, v_{i(j+1)} v_{\ell(j+1)} - m_{i\ell}\, v_{i(j)} v_{\ell(j)}] \end{aligned} \tag{A.3}$$

dissipated energy,

$$\begin{aligned} \Delta E_{Di} &= \frac{\Delta t}{2}[c_{ii(j+1)}v_{i(j+1)}^2 + c_{ii(j)}v_{i(j)}^2] + \\ &\frac{\Delta t}{2}\sum_{\ell=1,\neq i}^{n} [c_{i\ell(j+1)}\, v_{\ell(j+1)} v_{i(j+1)} + c_{i\ell(j)}\, v_{\ell(j)} v_{i(j)}] \end{aligned} \tag{A.4}$$

potential energy,

$$\Delta E_{P_i} = \frac{1}{2} k_{ii(j+1)} u^2_{i\,(j+1)} - \frac{1}{2} k_{ii(j)} u^2_{i\,(j)} + \sum_{\ell=1,\,\neq i}^{n} [k_{i\ell(j+1)}\, u_{i(j+1)} u_{\ell(j+1)} - k_{i\ell(j)}\, u_{i(j)} u_{\ell(j)}] \tag{A.5}$$

as well as, external excitation energy

$$\Delta E_{Fi} = \frac{\Delta t}{2} [F_{i(j+1)} v_{i(j+1)} + F_{i(j)} v_{i(j)}] \tag{A.6}$$

Similarly to the case of single-degree free systems, by inserting equations (A.3) to (A.6) within the incremental form of energy balance relation (A.2) and then using Euler's formula, n-quadratic equations regarding velocity can be obtained as follows.

$$\begin{aligned}
&A_i v^2_{i(j+1)} + B_i v_{i(j+1)} + C_i = 0 \\
&A_i = m_{ii} + \Delta t c_{ii(j+1)} + k_{ii(j+1)} \Delta t^2 r^2 \\
&B_i = 2 \sum_{\ell=1,\,\neq i}^{n} m_{i\ell}\, v_{\ell(j+1)} + \Delta t \sum_{\ell=1,\,\neq i}^{n} c_{i\ell(j+1)}\, v_{\ell(j+1)} + \\
&2k_{ii(j+1)} \Delta t\, r\, u_{i(j)} + 2k_{ii(j+1)} \Delta t^2 r(1-r) v_{i(j)} \\
&+2\Delta t\, r \sum_{\ell=1,\,\neq i}^{n} k_{i\ell(j+1)} u_{\ell(j)} \\
&+2\Delta t^2 r(1-r) \sum_{\ell=1,\,\neq i}^{n} k_{i\ell(j+1)} v_{\ell(j)} + \\
&2\Delta t^2 r^2 \sum_{\ell=1,\,\neq i}^{n} k_{i\ell(j+1)} v_{\ell(j+1)} - \Delta t F_{i(j+1)} \\
&C_i = -m_{ii} v^2_{i(j)} - 2v_{i(j)} \sum_{\ell=1,\,\neq i}^{n} m_{i\ell}\, v_{\ell(j)} + \\
&\Delta t c_{ii(j)} v^2_{i(j)} + \Delta t v_{i(j)} \sum_{\ell=1,\,\neq i}^{n} c_{i\ell(j)}\, v_{\ell(j)} \\
&+ (k_{ii(j+1)} - k_{ii(j)}) u^2_{i\,(j)} - k_{ii(j+1)} \Delta t^2 (1-r)^2 v^2_{i(j)} + \\
&2k_{ii(j+1)} \Delta t (1-r) u_{i(j)} v_{i(j)} + \\
&2u_{i(j)} [\sum_{\ell=1,\,\neq i}^{n} (k_{i\ell(j+1)} - k_{i\ell(j)}) u_{\ell(j)} + \\
&\Delta t(1-r) \sum_{\ell=1,\,\neq i}^{n} k_{i\ell(j+1)} v_{\ell(j)} + \Delta t\, r \sum_{\ell=1,\,\neq i}^{n} k_{i\ell(j+1)} v_{\ell(j+1)}] \\
&+2v_{i(j)} [\Delta t(1-r) \sum_{\ell=1,\,\neq i}^{n} k_{i\ell(j+1)} u_{\ell(j)} + \\
&\Delta t^2 (1-r)^2 \sum_{\ell=1,\,\neq i}^{n} k_{i\ell(j+1)} v_{\ell(j)} + \\
&\Delta t^2 r(1-r) \sum_{\ell=1,\,\neq i}^{n} k_{i\ell(j+1)} v_{\ell(j+1)}] - \Delta t F_{i(j)} v_{i(j)}
\end{aligned} \tag{A.7}$$

Expressing previous relationships in large-scale structures in a matrix form will be suitable both in displaying equations and in computer programming. Hence, the decomposition of mass, damping, and stiffness matrices to two diagonal (D) and non-diagonal (ND) matrices is desirable as follows.

$$\begin{aligned}
&\mathbf{M} = \mathbf{M}_{D} + \mathbf{M}_{ND} \\
&\mathbf{C} = \mathbf{C}_{D} + \mathbf{C}_{ND} \\
&\mathbf{K} = \mathbf{K}_{D} + \mathbf{K}_{ND}
\end{aligned} \tag{A.8}$$

Eventually, the vectors consist of coefficients in quadratic Eq.(25) would be simplified as

$$\begin{aligned}
&\mathbf{A} = \mathrm{diag}(\mathbf{M}_{D} + \Delta t\, \mathbf{C}_{D\,(j+1)} + a_1^2 \mathbf{K}_{D\,(j+1)}) \\
&\mathbf{B} = \mathbf{B}_{NC} + \mathbf{B}_{C} \\
&\mathbf{B}_{NC} = 2a_1 \mathbf{K}_{(j+1)} (\mathbf{u}_j + a_2 \mathbf{v}_j) - \Delta t \mathbf{F}_{(j+1)} \\
&\mathbf{B}_{C} = (2\mathbf{M}_{ND} + \Delta t\, \mathbf{C}_{ND\,(j+1)} + 2a_1^2 \mathbf{K}_{ND\,(j+1)}) \mathbf{v}_{(j+1)}; \\
&\mathbf{C} = \mathbf{C}_{NC} + \mathbf{C}_{C} \\
&\mathbf{C}_{NC} = \mathbf{v}_j . ([-(\mathbf{M} + \mathbf{M}_{ND}) + \Delta t\, \mathbf{C}_j + \\
&a_2^2 (2\mathbf{K}_{(j+1)} - 3\mathbf{K}_{D\,(j+1)})] \mathbf{v}_j + \\
&2a_2 \mathbf{K}_{(j+1)} \mathbf{u}_j - \Delta t \mathbf{F}_{(j+1)}) + 2\mathbf{u}_j . (\mathbf{K}_{(j+1)} - \mathbf{K}_j) \mathbf{u}_j \\
&\mathbf{C}_{C} = (2a_1 \mathbf{u}_j + 2a_1 a_2 \mathbf{v}_j) . \mathbf{K}_{ND\,(j+1)} \mathbf{v}_{(j+1)}
\end{aligned} \tag{A.9}$$

In these relationships, $a_1 = r\Delta t$ and $a_2 = (1- r)\Delta t$ are two parameters affected by the size of the time-step and integration scheme.

Appendix 2. Derivation of Exact Solution in Example 4.3 By Laplace Transform

The set of governing equations with zero initial conditions to be solved is

$$\begin{cases} 156\ddot{u}_1 - 13\ddot{u}_2 + 10\dot{u}_1 + 2\dot{u}_2 + 262.44u_1 + 131.22u_2 = H(t) \\ -13\ddot{u}_1 + 4\ddot{u}_2 + 2\dot{u}_1 + 4\dot{u}_2 + 131.22u_1 + 87.48u_2 = 0 \end{cases} \tag{A.10}$$

where the $H(t)$ denotes the Heaviside step function.
By taking Laplace Transform with defining $F=L(u_1)$ and $G=L(u_2)$ and imposing zero initial conditions, we have

$$\begin{cases} 156s^2F - 13s^2G + 10sF + 2sG + 262.44F + 131.22G = \dfrac{1}{s} \\ -13s^2F + 4s^2G + 2sF + 4sG + 131.22F + 87.48G = 0 \end{cases} \tag{A.11}$$

Where s is the transformation variable.
To obtain F and G functions, by solving Eq.(A.11)

$$\begin{cases} F = \dfrac{4s^2 + 4s + 87.48}{455s^5 + 716s^4 + 18144s^3 + 1399s^2 + 5739s} \\ G = \dfrac{13s^2 - 2s - 131.22}{455s^5 + 716s^4 + 18144s^3 + 1399s^2 + 5739s} \end{cases} \quad \text{(A.12)}$$

As we know from mathematics, in order to take the inverse Laplace transform, it would be appropriate to write these expressions in the form of partial fractions.

$$\begin{cases} F = \dfrac{0.01524}{s} + \dfrac{-0.00009s - 0.00018}{(s+0.7539)^2 + (6.2362)^2} + \\ \dfrac{-0.01514s - 0.00096}{(s+0.0328)^2 + (0.5644)^2} \\ G = \dfrac{-0.02286}{s} + \dfrac{-0.00091s - 0.00149}{(s+0.7539)^2 + (6.2362)^2} + \\ \dfrac{0.02377s + 0.00168}{(s+0.0328)^2 + (0.5644)^2} \end{cases} \quad \text{(A.13)}$$

Eventually, by taking the inverse transform, L^{-1}, and simplifying, the response of the system (u_1,u_2) can be computed

$$\begin{cases} u_1 = 0.0152 + \\ 0.000091\exp(-0.7539t)\cos(6.2362t - 3.3387) + \\ 0.01516\exp(-0.0328t)\cos(0.5644t - 3.0874) \\ u_2 = -0.0228 + \\ 0.00092\exp(-0.7539t)\cos(6.2362t - 3.2823) + \\ 0.02382\exp(-0.0328t)\cos(0.5644t - 0.0670) \end{cases} \quad \text{(A.14)}$$

Appendix 3. Finite Element Formulation of a Frame Element with Geometric Nonlinearity

With regard to (Reddy 2014[30]), a planar beam-column element is considered as shown in Figure 29(a). Generally, three DOFs (two transitions in the x-dir. and y-dir. along with one rotation about the z-axis) may be defined at two end nodes. This structural component is subjected to external loading, q(x) and f(x) respectively stand for transverse and longitudinal loads according to Figure 29(b).

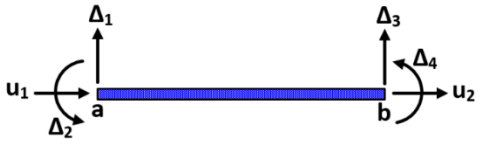

(a)

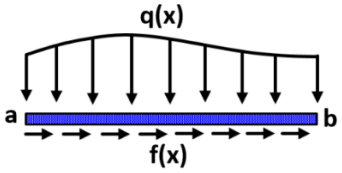

(b)

Fig. 29: A view of the frame element:
(a) Six DOFs defined for the element; (b) Applied loading.

So the whole degrees of freedom of this element can be expressed by $\{d^e\}=\{u_1, \Delta_1, \Delta_2, u_2, \Delta_3, \Delta_4\}$. Now, if we approximate the displacement field within the element, including axial displacement, $u(x)$, and transverse deformation, $u(x)$, by the interpolation functions (a.k.a shape functions) with Eq.(A.15).

$$u(x) = \sum_{i=1}^{2} \psi_i u_i \quad , \quad w(x) = \sum_{i=1}^{4} \phi_i \Delta_i \quad \text{(A.15)}$$

In which $\psi(x)$ and $\phi(x)$ functions can be obtained in terms of a dimensionless coordinate variable, $\xi=x/L$.

$$\begin{aligned} &\psi_1 = 1-\xi;\ \psi_2 = \xi; \\ &\phi_1 = 1-3\xi^2+2\xi^3;\ \phi_2 = \ell(1-2\xi^2+\xi^3); \\ &\phi_3 = 3\xi^2-2\xi^3;\ \phi_4 = \ell(-\xi^2+\xi^3) \end{aligned} \quad \text{(A.16)}$$

The nonlinear strain-displacement relationship by taking into account the large deformations under the Bernoulli's hypothesis (i.e., ignoring the distortional deformations) is expressed as follows.

$$\varepsilon_x = \underbrace{\frac{\partial u}{\partial x} + \frac{1}{2}\left(\frac{\partial w}{\partial x}\right)^2}_{Axial} - \underbrace{z\frac{\partial^2 w}{\partial x^2}}_{Bending} \quad \text{(A.17)}$$

Where the existence of $(\partial w/\partial x)^2$ denotes the nonlinear geometric effect (large deformation) in the present problem. Assuming linear behavior of the materials ($\sigma_x=E.\varepsilon_x$) one can express the strain energy stored in the element, U^e, as below.

$$U^e = \int_V \left(\frac{1}{2} E\varepsilon_x^2\right) dV \quad \text{(A.18)}$$

Besides, the potential energy, V^e, associated with the applied loads is also given by

$$V^e = \int_V (f.u + q.v)\, dV \quad \text{(A.19)}$$

Subsequently, the potential function ($\Pi^e=U^e-V^e$) and applying the *minimum total potential energy principle* ($\delta\Pi^e=0$) along with some mathematical simplification, the equilibrium equations of the system may be written in matrix form.

$$\begin{bmatrix} \mathbf{K}^{11} & \mathbf{K}^{12} \\ \mathbf{K}^{21} & \mathbf{K}^{22} \end{bmatrix} \begin{Bmatrix} \mathbf{\Delta}_1 \\ \mathbf{\Delta}_2 \end{Bmatrix} = \begin{Bmatrix} \mathbf{F}_1 \\ \mathbf{F}_2 \end{Bmatrix} \quad \text{(A.20)}$$

By definition:

$\boldsymbol{\Delta}_i^1 = u_i \quad for \quad i = 1, 2$ and $\boldsymbol{\Delta}_I^2 = \Delta_I \quad for \quad I = 1, 2, 3, 4$

these matrix and vectors are defined as follows.

$$\mathbf{K}_{ij}^{11} = \int_{x_a}^{x_b} EA \frac{d\psi_i}{dx} \frac{d\psi_j}{dx} dx;$$

$$\mathbf{K}_{iJ}^{12} = \frac{1}{2} \int_{x_a}^{x_b} EA \left(\frac{dw}{dx} \right) \frac{d\psi_i}{dx} \frac{d\phi_J}{dx} dx;$$

$$\mathbf{K}_{Ij}^{21} = \int_{x_a}^{x_b} EA \left(\frac{dw}{dx} \right) \frac{d\psi_i}{dx} \frac{d\phi_J}{dx} dx; \qquad \text{(A.21)}$$

$$\mathbf{K}_{IJ}^{22} = \int_{x_a}^{x_b} EI \frac{d^2\phi_I}{dx^2} \frac{d^2\phi_J}{dx^2} dx + \frac{1}{2} \int_{x_a}^{x_b} EA \left(\frac{dw}{dx} \right)^2 \frac{d\phi_I}{dx} \frac{d\phi_J}{dx} dx;$$

$$\mathbf{F}_i^1 = \int_{x_a}^{x_b} f(x)\psi_i dx; \quad \mathbf{F}_I^2 = \int_{x_a}^{x_b} q(x)\phi_I dx;$$

Note that the elements of the matrices $\mathbf{K}^{12}$, $\mathbf{K}^{21}$, and $\mathbf{K}^{22}$ are functions of the unknown variable, $w(x)$; therefore, it is necessary to update the stiffness matrix of the elements at any time in terms of the current geometry of the system by employing a trial and error process.